TRIASSIC STRATIGRAPHY IN THE ISLAND OF HYDRA (GREECE)

LUCIA ANGIOLINI, LUCA DRAGONETTI, GIOVANNI MUTTONI & ALDA NICORA

Riassunto. La successione sedimentaria di età triassica, che affiora sull'isola di Hydra, è costituita alla base da pochi metri di quarzareniti (Formazione di Aghios Nikolaos, Scitico), che passano gradualmente verso l'alto ad un'unità carbonatica molto spessa e ben diversificata, suddivisa in un membro e tre litozone (Calcare di Eros, Scitico-Pelsonico inf.).

Durante il Pelsonico la piattaforma del Calcare di Eros annega ed inizia la deposizione di una successione pelagica di età Pelsonico-Triassico sup., costituita da calcari nodulari (Calcare di Han Bulog) con tufiti verdi e da calcari con selce (Calcare di Adhami). Nella parte orientale dell'isola si sviluppa invece una spessa piattaforma carbonatica (Calcare di Pantokrator) di età Illirico-Triassico sup. La sovrastante successione pelagica, di età giurassica, segna il definitivo annegamento delle piattaforme triassiche e l'instaurarsi di condizioni bacinali. La successione triassica di Hydra rappresenta quindi una tipica successione di margine continentale passivo e suggerisce l'appartenenza di Hydra al dominio Subpelagoniano, nell'accezione di margine passivo occidentale della microplacca Pelagoniana.

Abstract. The Triassic sedimentary succession, cropping out in the island of Hydra, starts with a few metres of quartzarenites (Aghios Nikolaos Fm., Scythian) vertically making transition to a thick carbonate unit (Eros Lmst., Spathian-Pelsonian) subdivided into three lithozones and one member. During Pelsonian an extensional tectonic phase dissects the Eros carbonate platform. Its consequent downwarping results in the deposition of a pelagic sequence spanning the Pelsonian-Late Triassic time interval. This succession generally consists of few metres of nodular limestones (Han Bulog Lmst., Late Pelsonian-Early Ladinian) associated with green tuffs, followed by few hundred metres of cherty limestones (Adhami Lmst.). In the eastern part of the island a thick carbonate bank (Pantokrator Lmst.) develops, spanning the Illyrian to Late Triassic time interval. An overlying pelagic sequence, Jurassic in age, marks the downwarping of the Pantokrator carbonate platform. A typical passive continental margin succession is thus recorded in the Triassic of Hydra, suggesting its affinity with the Subpelagonian domain.

Introduction.

The island of Hydra emerges from the Aegean Sea a few miles south of the Argolis Peninsula (Fig. 1). Its sedimentary succession, spanning the Permian to Jurassic time interval, is considered very significant for unravelling the geologic history of this

part of the Hellenides. For many authors (see fig. 7, 40 in Jacobshagen, 1986) the island of Hydra belongs to the Pelagonian zone which consists of rocks of continental assemblage lying on a prealpine metamorphic basement. This zone is considered a south tethydean microplate differentiated in consequence of a Triassic rifting (Channel & Horvath, 1976; Dixon & Robertson, 1984; Mountrakis et al., 1987). Conversely
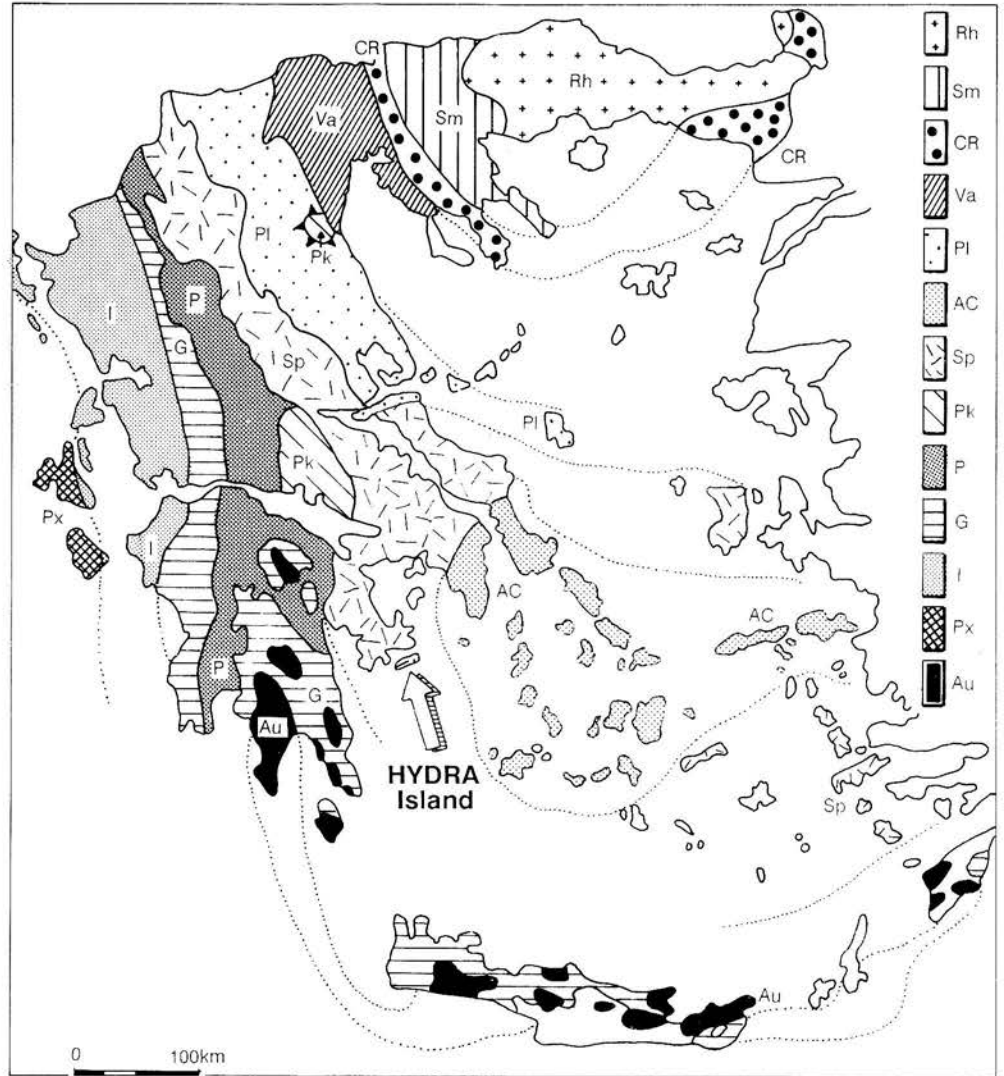
Fig. 1 - Structural zones of the Hellenides modified after Mountrakis et al. (1987). Rh) Rhodope; Sm) Serbomacedonian; CR) Circum Rhodope; Va) Vardar; Pl) Pelagonian; AC) Attico-cycladic; Sp) Subpelagonian; Pk) Parnasos; P) Pindos; G) Gavrovo Tripolis; I) Ionian; Px) Paxos; Au) Plattenkalk-Talea Ori.

Bender et al. (1960), Bannert & Bender (1968), Römermann (1968) locate the island of Hydra in the Subpelagonian zone. The latter, a zone placed to the west of the Pelagonian and striking parallel to it, is characterized by ophiolitic slices cropping out widely in the Argolis Peninsula. Finally, Jacobshagen (1977; 1989 pers. comm.) postulates that Hydra belongs to the Subpelagonian zone, considering it as a passive continental margin succession, deposited on the western part of the Pelagonian terrane. According to this interpretation the ophiolitic bodies are considered as allochthonous (Baumgartner, 1985).

The present paper provides an analysis of the Triassic succession of Hydra, depicts its geological history and gives further evidence to the interpretation of its affinity with the Subpelagonian domain in the sense of Jacobshagen, i.e. as a sedimentary succession of a passive continental margin.

A schematic geological map (scale 1:25.000) of Hydra is also included. The map is the result of the diploma thesis field work of L. Angiolini, L. Dragonetti and G. Muttoni during summers 1988 and 1990, with the supervision of M. Gaetani and A. Nicora.

Previous works.

The island of Hydra was mentioned for the first time in the reports of the "Expédition scientifique de Morée" (1834, 2:159) for its analogies with the Tripolitza series. In 1892 Philippson proposed a Cretaceous age for the rocks of Hydra.

From 1906 to 1955 Renz tried to reconstruct the stratigraphy of the island and published a map (1955). Particularly he studied the microfaunal associations (fusulinids, small foraminifers, Algae) as in also the brachiopods of Permian rocks outcropping along the southern coast of Hydra. In 1940, Okonomidis presented a geological map (1:100.000) of Hydra, essentially based on the studies of Renz. Haralambous (1963) described the Carboniferous-Triassic succession along a profile striking from the Gulf of Palamida to the southern coast of the island (see Fig. 3).

Römermann and Jacobshagen studied Hydra from 1961 to 1965 and in 1981 they published a geological map (IGME 1:50.000) and they recognized a Carboniferous-Jurassic sequence. In 1972 Grant studied the brachiopods of the Upper Permian limestones, demonstrating the correlation between the *Lyttonia* Limestone of Hydra and the *Productus* Limestone of Khisor Range and Salt Range (Pakistan).

In 1973 Wendt published a work on the Hallstatt (Bulog) Limestone of Jugoslavia and Greece. In Hydra he distinguished two different facies deposited in zones with different rate of subsidence during middle Anisian to Ladinian:
- the Aghia Marina Zone (south of Hydra), probably in temporary emergence during this time, as indicated by evidence of subaerial weathering at the top of Eros Limestone and by the local absence of the overlying Bulog Limestone;
- the Aghia Triada zone (north of Hydra), a faster subsiding basin characterized by a thicker and more continuous Bulog Limestone and by the presence of gravity
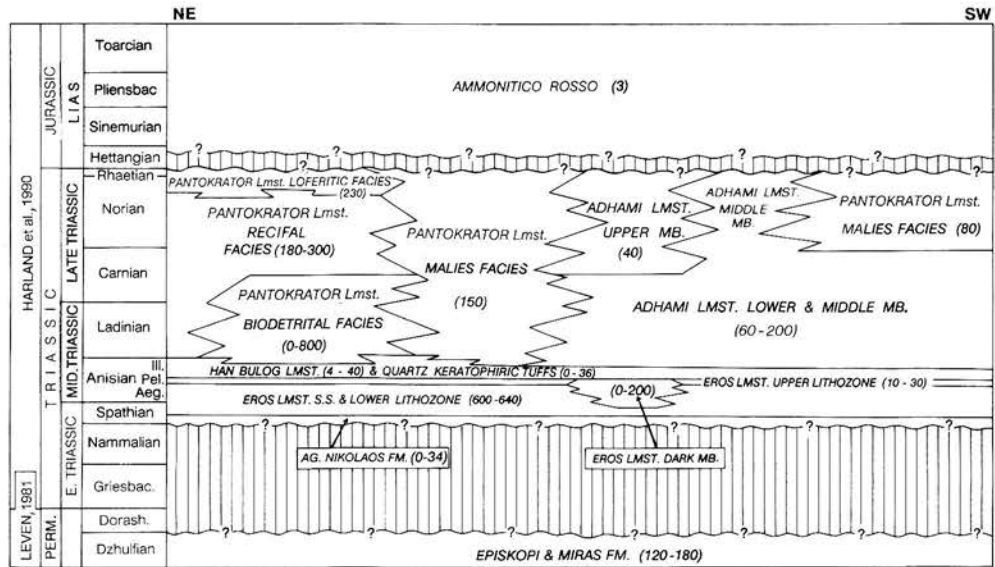
Fig. 2 - Stratigraphic scheme of Hydra.

flows coming from the Ag. Marina zone. During the Ladinian an environmental shift occurred, associated with emergence of the Ag. Triada zone and establishment of deep marine condition in Ag. Marina zone.

In 1984 Schäfer and Senowbari-Daryan studied the Upper Triassic sequence of Hydra. They identified three different facies within the carbonate platform of the Pantokrator Limestone. They also proposed a Late Triassic to Liassic age for this limestone, which prograded southward over the basinal succession of the Horsteinplattenkalk.

In 1986, Durkoop et al. published a report on Triassic red limestones of Argolis and Hydra. They pointed out that the Permian carbonate platform collapsed during Early Triassic with deposition of sandy gravity flows containing Permian and Schythian-Anisian calcareous blocks (Richter & Fuchtbauer, 1981). Near Episkopi, these gravity flows are thought to pass to red micritic sediments with an upper Scythian-lower Anisian conodont fauna.

In 1987, Nestell and Wardlaw worked out the conodont fauna of Upper Permian rocks of Hydra; they reported only lower Dzhulfian associations. The Permian sequence of Hydra has been recently studied in great detail by Baud et al. (1991) and by Grant et al. (1991).

Geological setting.

The sedimentary sequence of Hydra (Fig. 2) spans the Permian to Jurassic time interval. The northward homoclinal dip brings the Permian to crop out in the south-

1 O. Ompori thrust sheet
2 Southern thrust sheet
3 O. Zakoni thrust sheet
4 Kutali thrust sheet
5 Kastevas slice
a Limnionisa fault
b Alonaki fault
c Vlichos fault
d Palamida fault
e Episkopi fault
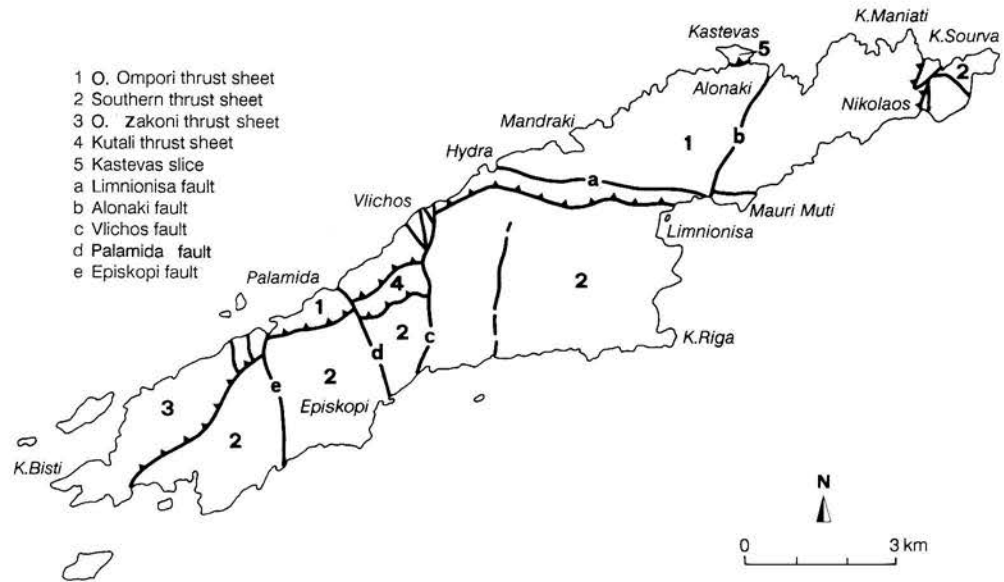
Fig. 3 - Tectonic map of Hydra showing the position of the principal thrust sheets and faults.

ern coast of the island and the Jurassic along the northern. The sequence is arranged in four major thrust sheets (Fig. 3 and the included geological map) and it is affected by folds and kinks. Other minor slices may also be distinguished. These thrust sheets are dislocated by transcurrent faults (lateral ramps), which may have a regional significance.

The northern or upper thrust sheets (O. Ompori, O. Zakoni and Kutali thrust sheets) (Fig. 4) contain mainly Triassic shallow water sediments and the Jurassic pelagic formations, whereas the southern or lower sheet contains Permian to Pelsonian shallow water sediments overlain by a Pelsonian to Jurassic pelagic succession. As already pointed out by Römermann (1968) and Durkoop et al. (1986), differences along an east-west transect exist too, with more pelagic successions outcropping westward.

The sedimentary succession

This paper focuses essentially on the Triassic succession. The units that were investigated include (Fig. 2): the uppermost Permian, the Triassic Aghios Nikolaos Formation, Eros Limestone, Han Bulog Limestone, Quartz keratophyric tuffs, Adhami Limestone, Pantokrator Limestone, and briefly the Jurassic formations.
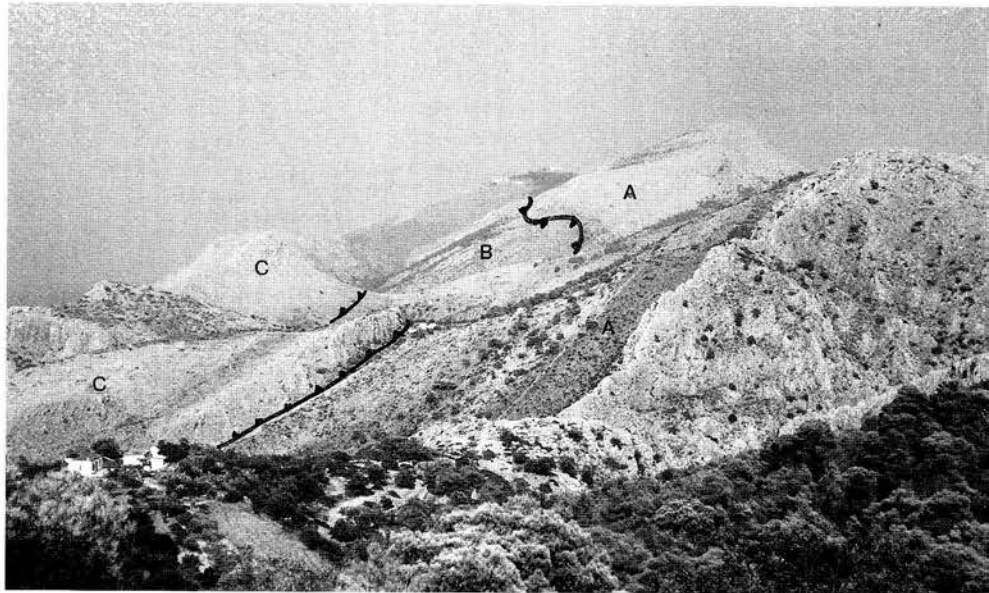
Fig. 4 - Photo from Gherakina to the East. From N to S: O. Ompori (C), Kutali (B) and southern thrust
        sheet (A).
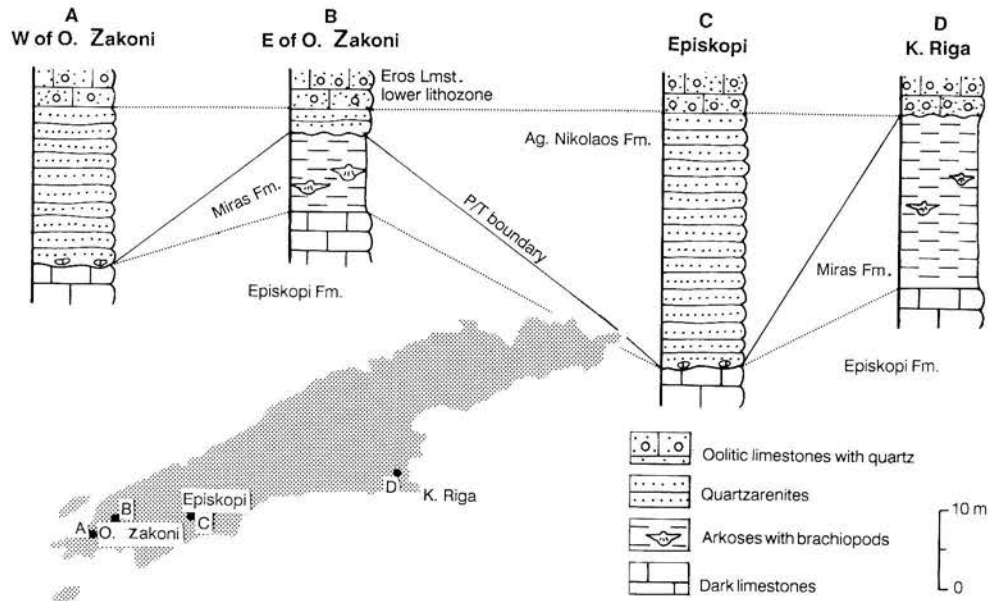
Fig. 5 - Stratigraphy of Permian-Triassic boundary and distribution of Miras and Ag. Nikolaos Forma-
        tions.

Uppermost Permian succession.

The Triassic succession overlies a Permian carbonate and terrigenous succession, which forms the oldest outcrops of the island and consists of three groups (from the base: Thikia Group, Klimaki Group and Barmari Group; nomenclature after Baud et al., 1991; Grant et al., 1991).

The youngest part of the Permian (Barmari Group of Baud et al., 1991, with minor change) is represented by Episkopi Formation consisting of dark packstones with fusulinids, small foraminifers, echinoderms, brachiopods, gastropods, bivalves, Algae and corals. In some places, it is overlain by the Miras Formation. This formation consists of fine arkoses with abundant feldspars (40-50% of the bulk composition), which are now weathered to fine grained micas and very few epimatrix, pseudomatrix and carbonate cement (5-6% of the bulk composition). Bioclastic limestone lenses with brachiopods, foraminifers and conodonts are also present, 600 m west of Gherakina,

Fig. 6 - Photo shot on the south-western slope of O. Zakoni showing limestone clasts at the base of Ag. Nikolaos Fm.

along the path to Kap Bisti, 200 m a.s.l. The brachiopods are chiefly represented by *Dictyoclostidae* (*Tyloplecta* sp.) and *Linoproductidae*. The petrography of the Miras Fm. is very similar to that of the other Permian terrigenous formations. In fact the Nisisa Fm. (Thikia Group of Baud et al., 1991) chiefly consists of arkoses and the Kap Bisti group p.p. consists of lithic greywackes. Instead there is a great difference in petrography between the Permian terrigenous and the Lower Triassic Ag. Nikolaos Fm., which consists of quartzarenites.

Fusulinid and small foraminifer associations indicate a Dzhulfian age for the Episkopi Formation. Furthermore the Dzhulfian conodont *Hindeodus julfensis* (Sweet) has been identified in the Miras Formation in the locality 600 m west of Gherakina.

The relationships between the formations at the Permian-Triassic boundary are very complicated because of lateral discontinuity of the Lower Triassic Ag. Nikolaos Fm. and of the Upper Permian Miras Fm. The contact is displayed at several localities (Fig. 5); from west to east:

- on the south-western slope of O. Zakoni, 220 m a.s.l., the boundary between the two sequences corresponds to an erosional surface developed between the Episkopi Fm. and the Ag. Nikolaos Fm., the latter containing clasts of the former at its base (Fig. 6);

- on the south-eastern slope of O. Zakoni a few metres of Ag. Nikolaos Fm. overlies the Miras Fm.;

- at Episkopi the contact is similar to that of the south-western slope of O. Zakoni;

- just behind the small house, at 140 m of altitude above K. Riga the boundary is located between the Eros Limestone (lower lithozone) and the Miras Fm. It is often sheared by faults.

Owing to the great differences in the petrography of Miras and of Ag. Nikolaos Fms. and to the presence of eroded clasts at the base of the latter, we can infer that there is a disconformity with a hiatus between the top of the Permian and the base of the Triassic sequences. This gap between Episkopi Fm. and Miras Fm. is not evident at the outcrop scale.

Aghios Nikolaos Formation.

The Ag. Nikolaos Fm., proposed in the present paper for the first time, was previously mapped as Permo-Triassic succession (Römermann et al., 1981) or included in the Miras Fm. (Baud et al., 1991). The appropriate name of this formation should have been Episkopi Fm. (from the type-section in Episkopi), but this name has been used by Baud et al. (1991) and Grant et al. (1991) to indicate a Late Permian formation. The name Ag. Nikolaos derives from a small bay on the north-western coast of the island, where the two lithologies, which characterize the formation, crop out.

The Ag.Nikolaos Formation chiefly consists of quartzarenites pinching out laterally in yellow siltstones, which belong to a distinct member mapped as Silty Member.

The maximum thickness of the Ag. Nikolaos Formation is 34 m at Episkopi, where the unit is exclusively sandy. The Silty Member, which crops out in the westernmost part of the island, is up to 30 m-thick.

This formation lies either above the Episkopi Formation or on the Miras Formation, whereas its top is delimited by the lower lithozone of the Eros Limestone. This contact is gradual with a progressive increase in oolites in the quartzarenites.

Lithology and petrography. The lithology of the Ag. Nikolaos Formation consists of well cemented, white to brown colored quartzarenites arranged in dm to m-thick beds, locally with cross laminations.

The petrographical analysis classifies the arenites as quartzwackes (QFR diagram). The main mineralogical component is polycrystalline and monocrystalline quartz (95%-99% of the grains), in subrounded grains occasionally showing undulose extinction. Phyllosilicates, Fe oxides and igneous rock fragments are also present. The matrix (30% of the bulk composition) consists of calcium carbonate cement, epimatrix and detritic matrix. These data point to high mineralogical and low textural maturities. Consequently these sandstones may be easily distinguished from the arkose of the Miras Fm.

The type-section was measured 500 m east of Episkopi at 200 m a.s.l. It consists of 30 cm to 1 m-thick strata of coarse sandstones yellow to white in coulor, with planar and cross laminations. In the first 2 m of the section light grey limestone clasts are included in the sandstones. The total thickness of the formation is 34 m.

The type-locality for the Silty Member is Kap Bisti.

Age. Owing to the lack of fossils, the age of this formation can be inferred only on the base of the stratigraphic position. The presence of local erosions at the contact between the Permian sequence and the Ag. Nikolaos Fm., the great difference in petrography from the Miras Fm. and its continuity with the overlying Eros Lmst. suggest that the Ag. Nikolaos is a transgressive detrital body at the base of the Triassic cycle.

Depositional environment. The sedimentary structures, i.e. cross laminations at low angle and pinching out of the sandy bodies in the siltstones, suggest that the depositional environment of this formation is probably a terrigenous marine flat affected by waves and/or by current action.

In fact the waves rework the detrital grains giving origin to litoral sand bars, whereas in the western part of Hydra an alluvional mud flat developes (Silty Mb.).

Eros Limestone (Römermann, 1968).

The Eros Limestone constitutes a huge carbonate bank, named after the highest mountain of Hydra by Römermann (1968). In this paper, for the first time, the Eros Lmst. has been subdivided and mapped into four subunits, whose rank was stated on

The maximum thickness of the Ag. Nikolaos Formation is 34 m at Episkopi, where the unit is exclusively sandy. The Silty Member, which crops out in the westernmost part of the island, is up to 30 m-thick.

This formation lies either above the Episkopi Formation or on the Miras Formation, whereas its top is delimited by the lower lithozone of the Eros Limestone. This contact is gradual with a progressive increase in oolites in the quartzarenites.

Lithology and petrography. The lithology of the Ag. Nikolaos Formation consists of well cemented, white to brown colored quartzarenites arranged in dm to m-thick beds, locally with cross laminations.

The petrographical analysis classifies the arenites as quartzwackes (QFR diagram). The main mineralogical component is polycrystalline and monocrystalline quartz (95%-99% of the grains), in subrounded grains occasionally showing undulose extinction. Phyllosilicates, Fe oxides and igneous rock fragments are also present. The matrix (30% of the bulk composition) consists of calcium carbonate cement, epimatrix and detritic matrix. These data point to high mineralogical and low textural maturities. Consequently these sandstones may be easily distinguished from the arkose of the Miras Fm.

The type-section was measured 500 m east of Episkopi at 200 m a.s.l. It consists of 30 cm to 1 m-thick strata of coarse sandstones yellow to white in coulor, with planar and cross laminations. In the first 2 m of the section light grey limestone clasts are included in the sandstones. The total thickness of the formation is 34 m.

The type-locality for the Silty Member is Kap Bisti.

Age. Owing to the lack of fossils, the age of this formation can be inferred only on the base of the stratigraphic position. The presence of local erosions at the contact between the Permian sequence and the Ag. Nikolaos Fm., the great difference in petrography from the Miras Fm. and its continuity with the overlying Eros Lmst. suggest that the Ag. Nikolaos is a transgressive detrital body at the base of the Triassic cycle.

Depositional environment. The sedimentary structures, i.e. cross laminations at low angle and pinching out of the sandy bodies in the siltstones, suggest that the depositional environment of this formation is probably a terrigenous marine flat affected by waves and/or by current action.

In fact the waves rework the detrital grains giving origin to litoral sand bars, whereas in the western part of Hydra an alluvional mud flat developes (Silty Mb.).

Eros Limestone (Römermann, 1968).

The Eros Limestone constitutes a huge carbonate bank, named after the highest mountain of Hydra by Römermann (1968). In this paper, for the first time, the Eros Lmst. has been subdivided and mapped into four subunits, whose rank was stated on

respect to the microfacies of the southern thrust sheet (Tab. 1). In the silty beds bivalves such as *Unionites* sp. and *Eumorphotis* sp. occur (det. R. Posenato).

Age. The presence of species of the genera *Unionites* and *Eumorphotis* similar to Lower Triassic species (Posenato, 1989 pers. comm.) suggests a late Early Triassic age for the lower lithozone, in agreement with the occurrence of *M. pusilla.* Durkoop et al. (1986) reported the occurrence of red micritic sediment with an Upper Scythian-Lower Anisian conodont fauna in the lower lithozone near Episkopi. We have sampled more than 20 kilos of red nodular limestone at Episkopi and near Vlichos in the same stratigraphic position, but unfortunately no conodonts were found.

Depositional environment. The lower lithozone represents the beginning of carbonate sedimentation in the Early Triassic. The depositional environment of this lithozone is interpreted as an oolitic bars field growing on a terrigenous flat (Ag. Nikolaos Fm.). The quartz input continues during bars growth. The microfacies of the

Fig. 7   -   Nodular limestone in the lower lithozone of Eros Lmst. (first valley west of Vlichos).

northern thrust sheets suggests deposition in a quiet environment; lower energy is confirmed by the presence of interbedded silty horizons. The major amount of quartz grains is probably due to the proximity to the area of erosion. Conversely in the southern thrust sheet the presence of oolites of different size and graded beds suggest an higher energy medium characterized by wave and\or currents. The growing and moving of the oolitic bars prevent the life of benthic organisms.

	Algae	Echinoderms	Gastropods	Bivalves	M.pusilla	G.shengi	M.dinarica	P.densa	E.wirzi	P.judicariensis	Duostominidae	G.grandis	P.globosa	Peloids	Problematica	Small Oolites	Large Oolites	More quartz	Less quartz
EROS LMST. s.s. Microfacies D2	X	X					X	X	X		X				X				
EROS LMST. s.s. Microfacies A1, B3, C3, C4, D1	X	X	X	X			X	X	X	X	X	X	X	X	X				
EROS LMST. s.s. Microfacies B2		X												X			X		
EROS LMST. s.s. Microfacies B1, C1, C2		X			X	X									X	X			
EROS LMST. lower lithoz. Northern thrust sheets	X	X	X	X	X	X										X		X	
EROS LMST. lower lithoz. Southern thrust sheet	X	X	X	X													X		X

Tab. 1 - Bioclastic, oolitic and detritic content detected in Eros Lmst. Among bioclasts the most significative foraminifers are listed.

Eros Limestone sensu stricto.

The Eros Lmst. s.s. is widely distributed in the island (Fig. 8 and geological map), outcropping from Kap Bisti to Molos in O. Zakoni thrust sheet and between the Palamida and Vlichos faults in the Kutali thrust sheet (Fig. 3). Moreover it constitutes the backbone of the southern thrust sheet. The maximum thickness of Eros Limestone s.s. varies from 500 to 600 m. It is overlain by the upper lithozone and passes laterally into the Dark Member.

Lithology and microfacies. The lithology is represented by massive beds of oolitic and bioclastic limestone. Fibrous cement has been mainly observed in the medium and upper portion of the Eros Lmst. s.s. The lithology has been fully studied along four north-south sections with the help of microfacies analysis (Fig. 8); from west to east they are as follow:

A) section south of Gherakina (samples H50-68). This section is located on the plateau immediately south of Gherakina, from 240 m a. s.l. to the houses of the small
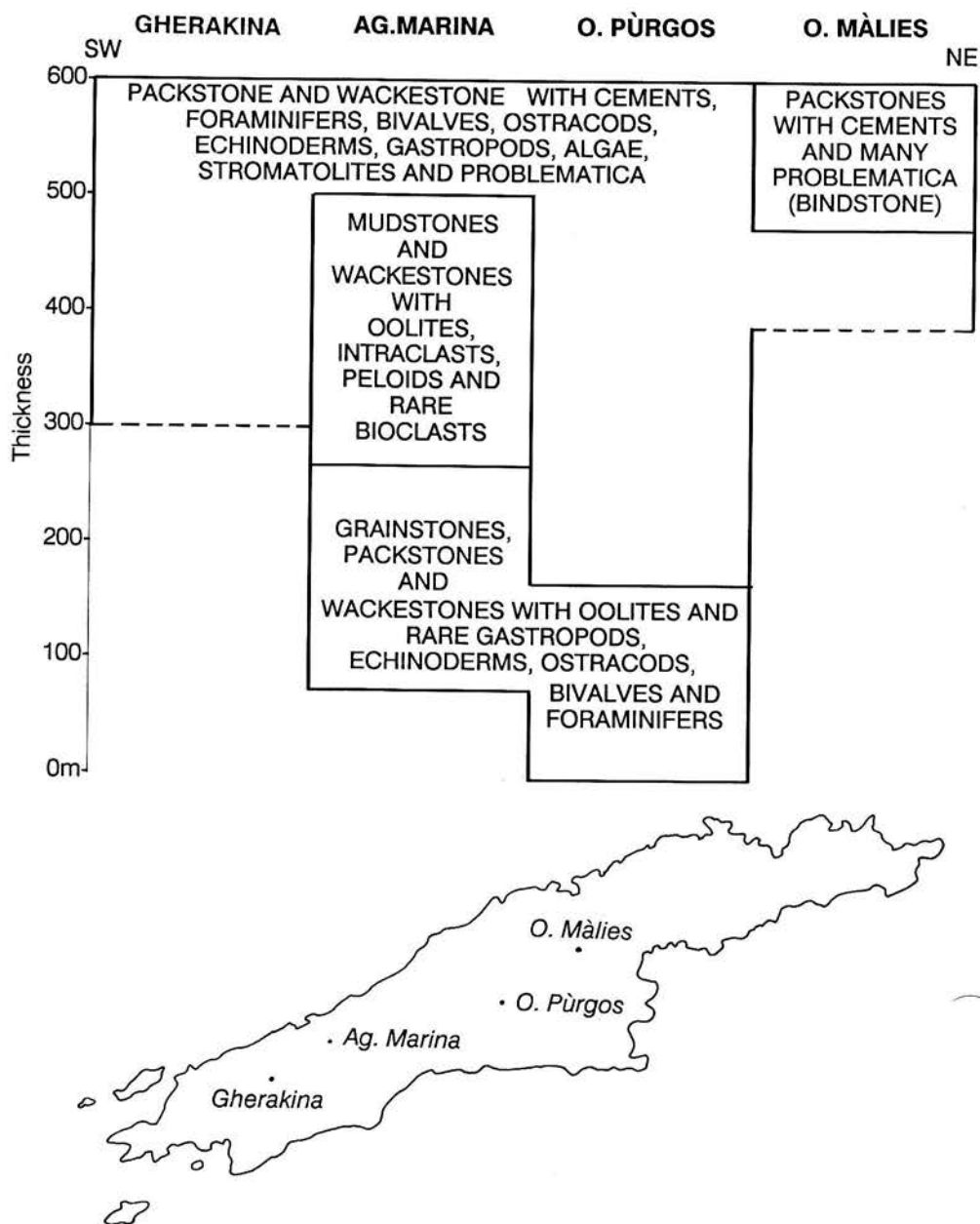
Fig. 8 - Internal subdivisions of Eros Lmst. s.s.: areal distribution and thickness of the microfacies.

village. The base of this section has not been sampled. Samples coming from the upper 300 m of the Eros Lmst. s.s. chiefly consist of recrystallized bioclastic packstones with fibrous cements (microfacies A1). Among the bioclasts there are proble-matica [*Tubiphytes obscurus* Maslov, *T. carinthiacus* (Flügel), *T. gracilis* Schäfer & Senowbari-Daryan, *Archaeolithoporella* sp., *Bacinella irregularis* Radoicic], Algae (*Cayeuxia* sp. and some dasyclads) and foraminifers [*Trochammina* sp., *T. jaunensis* Brönnimann & Page, *Pilammina densa* Pantic, *Meandrospira* sp., *M. dinarica* Kochansky-Devidé & Pantic, *Pseudobolivina* sp., *P. globosa* Kristan-Tollmann, *Endothyranella* sp., *E. wirzi* (Koehn-Zaninetti), *Tetrataxis* sp., *T. nana* Kristan-Tollmann, *Ophthalmidium* ? *chialingchiangense* (Ho), *Glomospirella* sp., *Neoendothyra* cf. *reicheli* Reitlinger and *Duostominidae*]. Bivalves, ostracods and echinoderms are also present.

B) Aghia Marina section (samples GL309-346). This section is located along the path from the village of Episkopi to Ag. Marina chapel and it starts at about 180 m a.s.l. Three microfacies have been recognized, from the base of Eros Lmst. s.s. to the top:

- microfacies B1 (200 m thick): oolitic grainstones with few bioclasts and lumps. The oolites are irregular in shape and surficial, small, homogeneous in sorting, sometimes flattened and oriented. Among the bioclasts, echinoderms, bivalves and foraminifers (*Tolypammina* sp. and *Ophthalmidium* sp.) have been detected;

- microfacies B2 (230 m thick): mudstones, wackestones and more rarely packstones and grainstones with small, surficial and irregular oolites, intraclasts, peloids and rare bioclasts as sponges, echinoderms and the foraminifer *Glomospira* sp.;

- microfacies B3 (100 m thick): wackestones and packstones with bioclasts and peloids. Among the bioclasts there are calcareous sponges, echinoderms, dasycladacean Algae, bivalves, stromatolites, oncolites and foraminifers [*Glomospira* sp., *Meandrospira dinarica*, *Pilammina densa*, *Tolypammina gregaria* Wendt, *Palaeomiliolina judicariensis* (Premoli Silva), "*Earlandinita*" sp., *Glomospirella* cf. *grandis* (Salaj), *Endothyra* sp., *Textulariidae* and *Duostominidae*].

C) O. Purgos section (samples H102-131/GL57-68). This section extends from 240 m a.s.l. on the southern slope of O. Purgos to 340 m a.s.l. on the northern slope, through the summit. Four microfacies have been recognized, from the base of Eros Lmst. s.s. to the top:

- microfacies C1 (40 m thick): strongly recrystallized bioclastic wackestones with ostracods and few foraminifers (*Meandrospira pusilla*);

- microfacies C2 (135 m thick): oolitic packstones and grainstones with some lumps and intraclasts. Among the bioclasts, echinoderms, foraminifers (*Meandrospira* sp.) and problematica (*Tubiphytes obscurus*) have been detected;

- microfacies C3 (50 m thick): recrystallized bioclastic packstones with fibrous cements. The bioclasts include echinoderms, problematica (*Tubiphytes obscurus* and *T. carinthiacus*) and foraminifers (*Endothyranella* sp., *Meandrospira dinarica*, *Glomospirella grandis*);

- microfacies C4 (more than 300 m thick): packstones and more rarely wacke-
stones with bioclasts and peloids. Macroscopic, fibrous and palisade cements arranged
in concentric bands are also present. The bioclasts include bivalves, echinoderms, os-
tracods, gastropods, rare problematica (*Tubiphytes obscurus*, *Bacinella irregularis* and
Archaeolithoporella sp.), Algae (*Oligoporella* sp. and *Solenopora* sp.) and foraminifers
(*Meandrospira dinarica*, *M. deformata* Salaj, *Endothyranella* sp., *E. wirzi*, *Mean-
drospiranella samueli* Salaj, *Pilammina densa*, *Tolypammina gregaria*, *Tetrataxis nana*,
"*Earlandinita*" sp., *Involutina* sp., *Calcitornella* sp., *Ammobaculites* sp., *Pseudobolivina*
sp., *Trochammina* sp., *Neoendothyra* sp., *Turrispirillina prealpina* Zaninetti & Brönni-
mann, *Glomospirella grandis*, *Duostominidae* and *Lagenidae*).

D) O. Malies section (samples H167-184). This section is located along the new
road striking from about 150 m of altitude above Kap Riga to the pass (200 m a. s.l.)
north of Limnionisa Ormos. The base of the Eros Lmst. s.s. along this section has not
been sampled. In the upper 200 m of the platform two microfacies have been detected.
From bottom to top:

- microfacies D1 (90 m thick): bioclastic packstones with cements and pellets.
Among the bioclasts there are echinoderms, gastropods, bivalves, ostracods, proble-
matica (*Bacinella irregularis*, *Tubiphytes obscurus*, *Archaeolithoporella* sp.) and
foraminifers (*Ammobaculites* sp., *Trochammina* sp., *Endothyra* sp., *Endothyranella* sp.,
Ophthalmidium ? *chialingchiangense*, *Neoendothyra* cf. *reicheli* and *Duostominidae*);

- microfacies D2 (120 m thick): bioclastic packstones with very abundant fibrous
cements. The bioclasts include echinoderms, ostracods, abundant *Tubiphytes obscurus*,
Bacinella irregularis, *Cayeuxia* sp. and foraminifers such as *Endothyranella* sp., *E. wirzi*,
Neoendothyra cf. *reicheli*, *Meandrospira dinarica*, *Pilammina densa*, *Trochammina* sp.,
Ammobaculites sp., *Duostominidae*. Owing to the presence of abundant *T. obscurus*
with evident encrusting fibrous cement, this rock can be classified as a bindstone.

The distribution of the major components of these microfacies is reported in
Tab. 1.

Age. The age of Eros Limestone s.s. has been determined on the base of
foraminifer and conodont associations. The lower portion of the platform lacks a sig-
nificant foraminifers association. However the presence of *M. pusilla* indicates an Early
Triassic age (Salaj et al., 1983 and Oravecz-Scheffer, 1987). Moreover we found Scy-
thian conodonts [*Neospathodus homeri* (Bender)] at about 310 m above the base of Eros
Lmst. s.s. on the eastern slope of O. Zakoni (MR 225 sample of M. Richards,
Lausanne, collected at the top of the Dark Mb.). In the upper part of Eros Limestone
the foraminifers association (*M. dinarica*, *P. densa*, *E. wirzi*, *P. iudicariensis*) may indi-
cate a Pelsonian age (Salaj et al., 1983 and Oravecz-Scheffer, 1987). The presence of
Lower to Upper Pelsonian conodonts (sections A, C, F) (Fig. 10, 11) in the upper
lithozone restricts to the Early Pelsonian the age of the top of the Eros Limestone s.s.
So almost the lower 300 m of the platform deposited during Late Scythian (Spathian)
and only the upper part is Anisian (up to Early Pelsonian).

Depositional environment. The depositional environment of the lower 200 m of the Eros Limestone (microfacies B1 and C2) is interpreted as migrating oolitic bar fields, probably affected by current winnowing, as shown by the homogeneity in sorting of the oolites. Higher in the sections, the oolitic fields are replaced by a lower energy environment, represented by bioclastic packstones with abundant foraminifers and cements (microfacies A1, B3, C3, C4, D1). At Ag. Marina, no foraminifers occur in the lower 200 m (microfacies B2) that represent lower energy environment. In the easternmost section (O. Malies), the foraminifer-bearing packstones are bound by very abundant *Tubiphytes* and algal crusts and encrusted by fibrous and palisade cements (microfacies D2). This suggests the existence of a hard, although poorly developed organic rim in the eastern part of the island. So during Scythian-Early Anisian a thick carbonate platform developes, consisting of oolitic bars at the base and open lagoon facies towards the top. The margin of the platform is probably located in the east, where bindstones are detected. Moreover this bank is dissected by intraplatform troughs, in which the Dark Mb. of the Eros Lmst. deposits.

Eros Limestone, Dark Member.

The Dark Member outcrops from Kap Bisti to Ormos Ag. Nikolaos, around the summit of O. Zakoni and east of the large valley west of Ormos Molos in O. Zakoni thrust sheet. It also constitutes the Kutali thrust sheet and it outcrops east of Ormos Limnioniza in the southern thrust sheet (see geological map). The thickness of this member varies widely, because of its interfingering to the Eros Limestone s.s. The maximum thickness measured is 200 m. The Dark Member is overlain either by the Eros Limestone s.s. or by the Han Bulog Limestone in the area north of O. Zakoni. Laterally the Dark Member makes a gradual transition to the platform. The transitional facies consists of massive, dark, sometimes brecciated limestones with few oolites and oncolites. The lithology and microfacies of the Dark Mb. have been studied in particular on the southern slope of O. Zakoni, in the valley west of Ormos Molos, in the first valley west of Vlichos and near Ormos Limnioniza.

Lithology. The lithology of the Dark Member consists of centimetric to decimetric laminated planar beds of dark limestone with chert in nodules and bands (Fig. 9a). Massive beds of intraformational breccias are also present. A later dolomitization replaced the primary laminated limestone and constitutes also the cement of the breccias (Fig. 9b).

Microfacies. The microfacies of the Dark Member chiefly consists of a thin alternation of mudstones and bioclastic wackestones with rare oolites and peloids. The bioclasts include pelagic bivalves, radiolarians, sponges spicules, rare echinoderms and foraminifers (*Glomospirella* sp., *Pilammina inconstans* Michalik, Jendrejakova & Borza, *Rectocornuspira kalhori* Brönnimann, Zaninetti & Bozorgnia, *Glomospirella triphonensis* Baud, Zaninetti & Brönnimann).

Age. The age of the Dark Member ranges from Spathian to Early Pelsonian according to the occurrence of *R. kalhori* in its lower part, of Spathian conodonts (*N.*
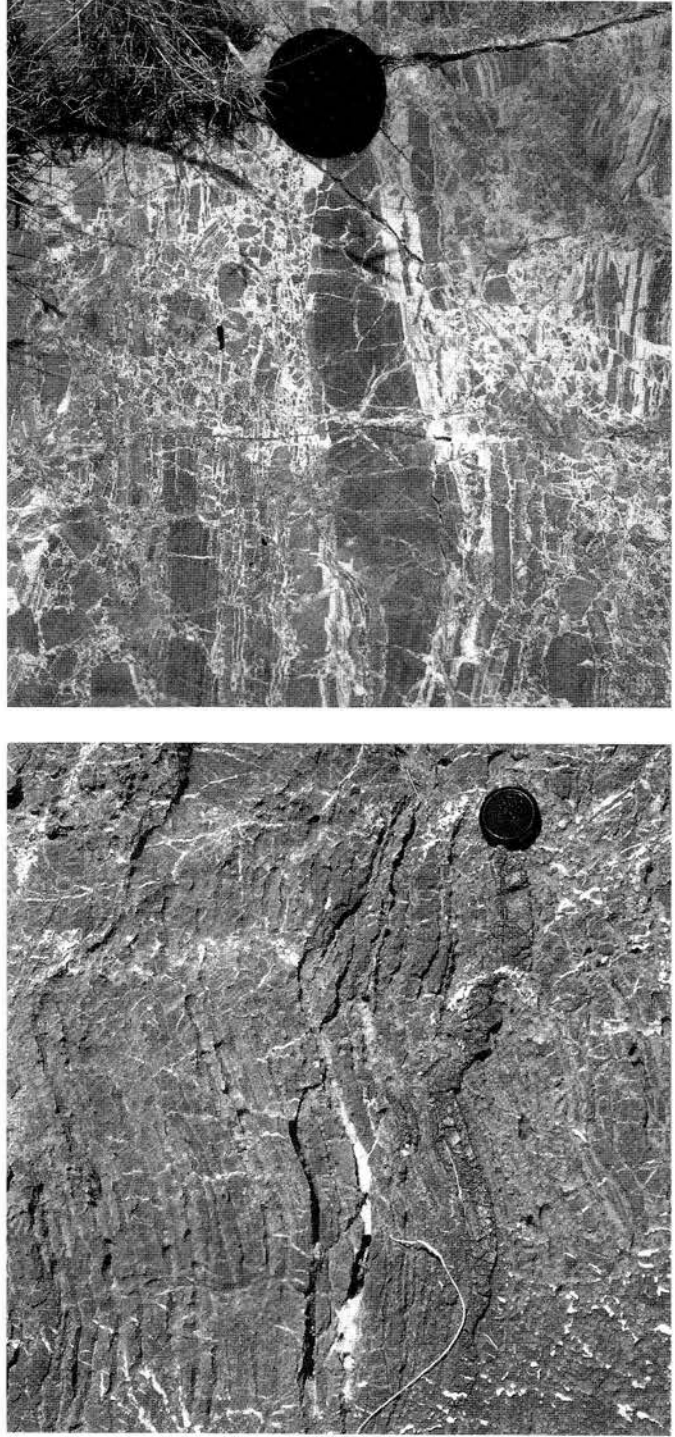
Fig. 9a, b - Photo of the Dark Member of Eros Lmst. (first valley west of Vlichos). 9a) Chert lenses; 9b) dolomitic intraformational breccias.

homeri) and of Pelsonian-Illyrian conodonts in the overlying Han Bulog Limestone (sections A, B, C, F, G, H) (Fig.10, 11) and to the relationship with the Eros Lmst. s.s.

Depositional environment. Owing to its discontinuous distribution, to its peculiar lithology and to the clear relation of interfingering with the Eros Lmst. s.s., the depositional environment of the Dark Member can be interpreted as intraplatform troughs. These troughs, anoxic but probably not very deep, developed in different sites either at the base of the platform, or in the middle, or from a hundred of metres over the base to the top of the Eros Lmst. s.s. The presence of both platform clasts (oolites and benthic foraminifers) and pelagic bioclasts (radiolarians and filaments), in the same discrete levels in the Dark Mb., indicates an episodic influx of open marine waters that sweep the platform and resedimented material into the basins. The abundance of intraformational breccias may suggest block-faulting activating the basins.

Eros Limestone, upper lithozone.

The thickness of this lithozone varies from 10 up to 30 m. In the northern thrust sheets the upper lithozone is overlain by the Han Bulog Limestone and locally by the Quartz-keratophyric tuffs. In the southern thrust sheet, the upper lithozone is overlain either by the Han Bulog Limestone, by the Quartz-keratophyric tuffs or by the Adhami Limestone, lower member. The breccias of the upper lithozone pass progressively upward into the Han Bulog Limestone. This is indicated by the occurrence of nodular limestones (similar to the Han Bulog Limestone) in the breccias.

Lithology. The lithology of this member consists of red matrix-bearing calcareous breccias with centimetric to decimetric gray oolitic clasts and pink clasts with crinoids. In the uppermost portion of this lithozone, the clasts are locally coated with cherty crusts.

Microfacies. The microfacies of the clasts consist of packstones and wackestones with peloids and bioclasts such as echinoderms, sponges, dasyclad Algae, ostracods, pelagic bivalves and foraminifers (*Meandrospira dinarica, Pilammina densa, Endothyranella* sp., *E. wirzi, Ammobaculites* sp., *Trochammina* sp., *T. almtalensis* Köhen-Zaninetti, *Endothyra* sp., *Tetrataxis nana, Permodiscus* sp., *Duostominidae*). The red matrix contains ostracods and pelagic bivalves.

Age. A rich conodont fauna has been found in this lithozone in the stratigraphic sections A, C, F (Fig. 10, 11 and Tab. 2). The association is mostly dominated by the occurrence of *Gondolella bulgarica* (Budurov & Stefanov), *G. bifurcata bifurcata* (Budurov & Stefanov), *G. bifurcata hanbulogi* (Sudar & Budurov) and *Gladigondolella tethydis* (Huckriede). In the lower part (sect. C, samples GL85-87) *G. bulgarica* and *G. b. bifurcata* prevail, whereas *G. b. hanbulogi* becomes more frequent higher up (sect. C, samples GL88-91). Based upon these considerations this lithozone seems to cover the whole Pelsonian time interval.

Depositional environment. The breccias of the upper lithozone record the downwarping of the Eros Lmst. platform, which is also suggested by the presence of
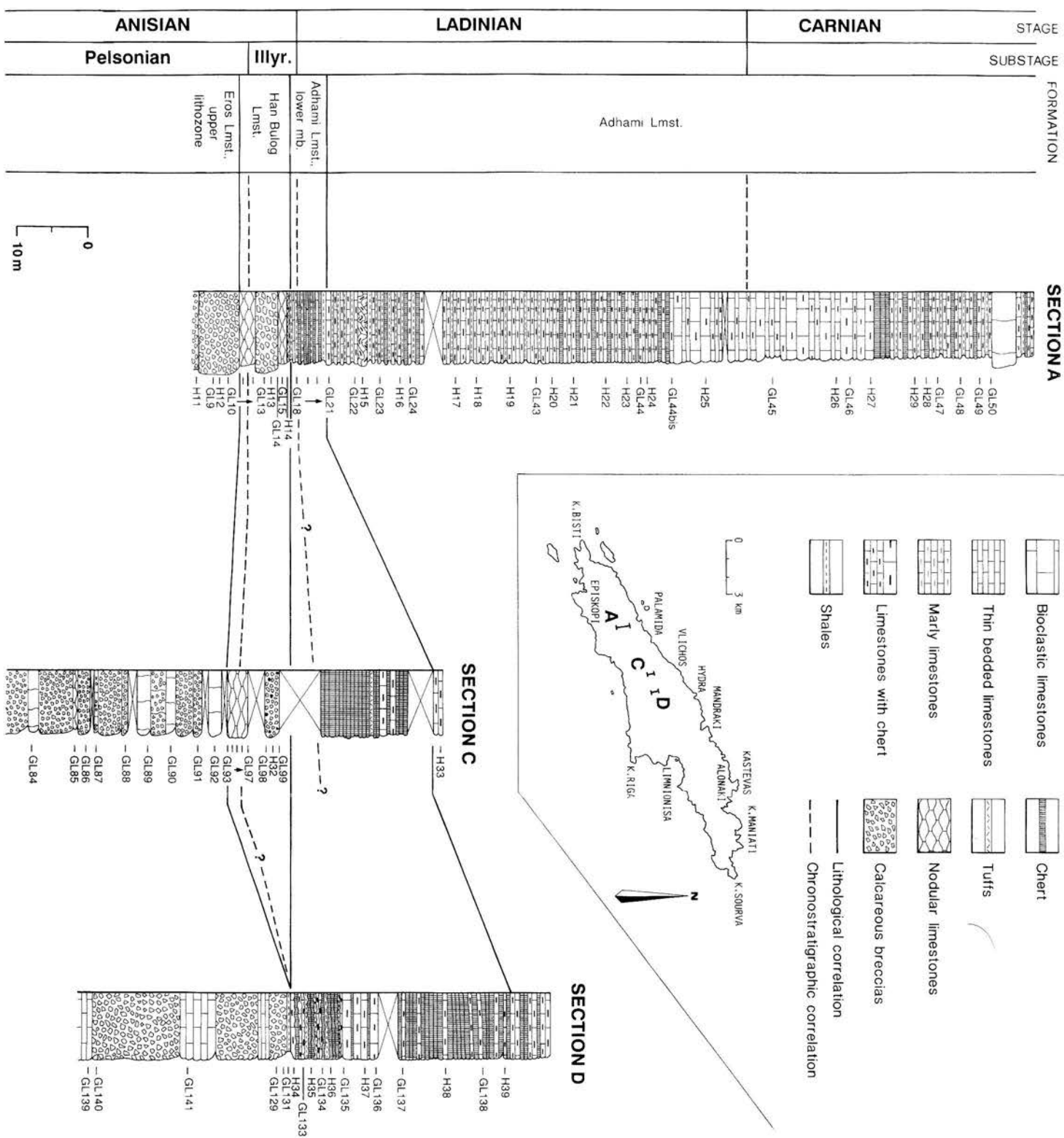
Fig. 10 - Detailed stratigraphic sections measured in the southern thrust sheet. Chronostratigraphic subdivisions and correlations based on conodont zonation. The locations of the sections are as follow: section A (central part of Hydra), from Ag. Marina chapel (180 m a.s.l.) northward for 200 m along the path to Ormos Palamida; section C (central part of Hydra), at 270 m a.s.l. on the ideal (by air) link between O. Eros and Vlichos; section D (central part of Hydra), at 240 m a.s.l. on the ideal (by air) link between O. Eros and Kamini, WNW of Pr. Ilia.

Fig. 11 - Detailed stratigraphic sections measured in the northern thrust sheets. Chronostratigraphic subdivisions and correlations based on conodont zonation. The locations of the sections are as follow: section B (central part of Hydra), along the right hydrographic side of the first valley west of Vlichos, from 40 m to 100 m a.s.l. in the O. Ompori thrust sheet; section E (western part of Hydra), along the western side of the second bay located east of the ideal (by air) link between O. Zakoni and the easternmost tip of Petasi Island; section F (western part of Hydra), along the first bay west of the ideal link between O. Zakoni and the easternmost tip of N. Petasi; section G (eastern part of Hydra), about 10 m south of the monastery located on the eastern side of the pass leading to Ormos Limnionisa from 240 to 250 m a.s.l. (the monastery is not located on the geological map); section H (eastern part of Hydra), 250 m WNW of Ag. Triados, from 175 to 180 m a.s.l.

L. Angiolini, L. Dragonetti, G. Muttoni & A. Nicora
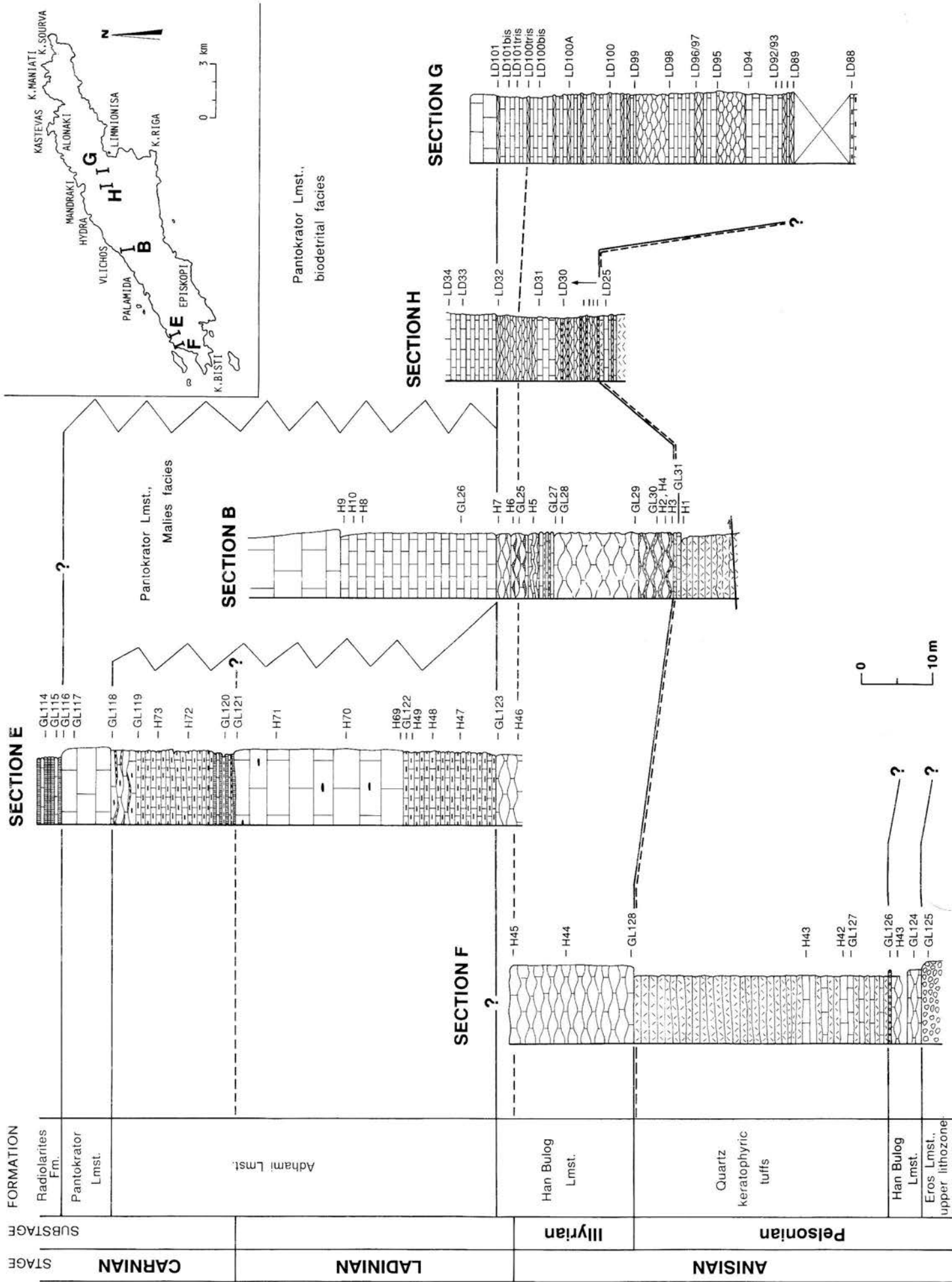
pelagic facies (Han Bulog Limestone and Adhami Limestone), above the upper litho-zone. The origin of these breccias is probably related to an increase of subsidence during the extensional phase begun in Late Scythian. In fact normal faults could have dissected the platform of Eros Lmst., causing the formation of huge bodies of breccias which show differences of thickness in short distance. Richter and Fuchtbauer (1981) suggest that the formation of breccias is due to a flexure of the platform caused by not homogeneous subsidence.

Han Bulog Limestone (Hauer, 1884).

This formation is known in the previous works on Hydra as the "Hallstatt facies" Limestone (Renz, 1906; Römermann et al., 1981). In 1931 Renz mapped it as Bulog Limestone. We prefer to indicate the formation with the full name of Han Bulog Limestone for its similarity and paleogeographical affinity with the Han Bulog Lmst. of the Dinarides, instead than the Hallstatt facies of the Northern Calcareous Alps.

The Han Bulog Lmst. consists of red and gray nodular limestone locally rich in ammonoids. The thickness of Han Bulog Lmst. varies depending on the thrust sheet it belongs. In the southern thrust sheet it is very discontinuous and reaches a maximum of 7 m, whereas in the northern sheets it varies from 20 to 40 m. The nature of the upper boundary of the Han Bulog Lmst. varies from place to place (see geological map):

- in the southern thrust sheet it is overlain by very thin and discontinuous Quartz keratophyric tuffs or by the Adhami Limestone, lower member;

- in O. Zakoni sheet (northern sheet; Fig. 3) it is bounded by the Adhami Lmst., whereas the Quartz keratophyric tuffs constitute a thick unit interbedded in the Han Bulog Lmst.;

- in the westernmost part of O. Ompori sheet (northern sheet; Fig. 3) the Han Bulog Lmst. is overlain by the Malies Facies of the Pantokrator Lmst., as can be seen in the Vlichos area. Here the transition is represented by 22 m of cm-thick beds of limestone with filaments and chert nodules. From Hydra-Chora towards the east (O. Ompori sheet) the Han Bulog Lmst. is bounded by the biodetrital and recifal facies of the Pantokrator Limestone.

Lithology. In the southern thrust sheet the lithology of the Han Bulog Lmst. consists of cm to dm-thick beds of red and gray nodular limestone locally with hard grounds and extremely rich in filaments, ammonoids (Fig. 12), crinoids and bivalves. The ammonites are imbricated and/or concentrated in lenses.

In the northern thrust sheets the lithology of this formation consists of cm to dm-thick beds of:

- red nodular limestone with nodules wrapped with red clay locally rich in ammonoids;

Fig. 12 - Photo of ammonoids of the Han Bulog Lmst. (first valley west of Vlichos).

- red nodular chert bearing limestone;
- gray limestone with filaments and very thin levels of red clay.

A few metres of breccias with probably Eros Limestone and Pantokrator Limestone clasts and filament-bearing clasts occur in the middle-upper part of this formation. These deposits are interpreted as representing episodes of resedimentation (mass-flows).

Microfacies. In the southern thrust sheet the microfacies consists of packstones and wackestones with abundant filaments. Radiolarians, echinoderms, ammonites, thin shelled gastropods, bivalves and benthic foraminifers have also been observed. The filaments lay in discrete levels bounded by stilolites. The valves are often disarticulated, sometimes broken and imbricated, probably due to current action. In the northern thrust sheets the microfacies is very similar, but usually the filaments are not imbricated and there is no sedimentological evidence for current action.

The bioclasts include foraminifers [*Meandrospiranella samueli* Salaj, *Meandrospira* sp., *Ammobaculites* sp., *Planiinvoluta* sp., *Reophax* sp., *Earlandinita* sp., *Ammodiscus* sp., *Valvulina* sp., *V. metula* (Kristan-Tollmann), *Pseudonodosaria* sp., *P. striatoclavata* (Spandel), *Duostominidae*], problematica (*Archaeolithoporella* sp., *Tubiphytes obscurus*, *Microtubus* sp.) and Algae (*Cayeuxia* sp., *Orthonella* sp., *Cladogirvanella cipitensis* Ott, *Parachaetetes* sp., *Solenoporaceae* and *Porostromata* sensu Pia). These deposits are interpreted as resedimented material from the rising platform of Pantokrator Limestone.

Lithified clasts with echinoderms, peloids and benthic foraminifers probably eroded from Eros Lmst. of the southern sheet, have also been detected.

Age. In 1931 Renz studied the ammonoids of the Han Bulog Lmst., suggesting an Illyrian age. We studied the rich conodont fauna. As shown in Fig. 10, 11 and Tab. 2, in the lower part of sections C (samples GL93-96) and F (samples GL124, H41) the association *G. bifurcata hanbulogi, G. bulgarica* and *Neospathodus kockeli* (Tatge) (present only in section C) points to a Late Pelsonian age.

In section B the lower conodont association above the Qz-keratophyric tuffs is still characterized by the presence of *Gondolella excelsa* (Mosher), *N. kockeli* (samples H1-3-4).

Higher up (sections A, B, F, G, H) (Fig.10, 11) the presence of *Gondolella constricta* Mosher & Clark, *G. excelsa* and *G.* aff. *szaboi* Kovacs and *G.* aff. *eotrammeri* Krystyn (LD95-LD45) testifies for Late Illyrian age. In section G (LD 100tris) the occurrence of *G. trammeri* Kozur at about 5 m below the top of the formation indicates an Early Ladinian age. This is also testified by the occurrence of *G. trammeri* at the top of section C (H33) (Fig. 10).

Based on these considerations the Han Bulog Limestone ranges from Latest Pelsonian to Latest Illyrian/Ladinian.

Depositional environment. Lithologic and microfacies analyses allow the following paleoenvironmental interpretations:

- in the southern thrust sheet the depositional environment of the Han Bulog Lmst. was characterized by a low rate of sedimentation, as indicated by the presence of hard-grounds. This unit was also deposited in a high energy environment with currents sweeping the bottom and leading to imbrication of the bivalves and ammonites. In agreement with Wendt (1973), who previously described these structures, the depositional setting is interpreted as a shallow water pelagic environment. The presence of mass-flows indicates slope gradients.

- In the northern thrust sheets the depositional environment is characterized by lower energy. The greater thickness and lateral continuity of the deposits indicate a probably more subsiding setting, but still lying in the photic zone environment. Furthermore the presence of material coming from the rising Pantokrator platform and from the lithified and eroded Eros Lmst. s.s. testifies that this deeper setting acted as a platform sediments trap.

Quartz keratophyric tuffs (Milch & Renz, 1911).

This formation consists of pale green and red acid tuffs, locally silicified. In the southern thrust sheet the tuffs form a thin (about 3 m), laterally discontinuous unit, lying on top of the Han Bulog Lmst. In the northern thrust sheets this formation locally constitutes a thicker unit (maximum 36 m), continuous and interbedded with the Han Bulog Lmst. (north-western coast).

These differences in thickness and lateral continuity are in agreement with the environmental interpretation previously depicted for the Han Bulog Lmst.

	G. bulgarica	G. constricta	G. b. hanbulogi	G. b. bifurcata	G. excelsa	G. cornuta	G. aff. szaboi	G. aff. eotramneri	G. tramneri	G. polygnathiformis	G. tadpole	G. foliata foliata	Gondolella sp.	N. kockeli	Gl. tethydis	Ozarkodina sp.	E. ziegleri	Prioniodella sp.	C. kochi
Section A																			
GL 50										X									
H 29											X								
GL 45											X	X							
GL 44 bis													X						
GL 24															X				
GL 17					X														
H 14								X											
GL 15																	X		
H 13															X				
GL 12					X								X			X			
GL 10	X	X													X				
Section B																			
H 10														X					
GL 27				X												X			
GL 29			X			X													
H 4					X										X				
H 3					X										X				
H 1	X			X	X									X					
Section C																			
H 33										X									
GL 97		X			X	X									X				
GL 96	X	X	X			X									X	X			
GL 95	X	X	X			X									X	X			
GL 94	X	X	X			X								X	X	X			
GL 93	X	X	X			X									X				
GL 91	X	X	X		X										X				
GL 90	X														X				
GL 88	X		X												X	X			
GL 87	X		X													X			
GL 86	X																		
GL 85	X																X	X	
Section D																			
H 37				X															
Section E																			
GL 118											X								
GL 119											X								
H 73											X								
GL 121												X							
H 48																			X
GL 123															X				
Section F																			
H 45					X				X										
H 44					X		X								X				
GL 127	X		X																
GL 124	X			X															
Section G																			
LD 101															X				
LD 101 bis												X							
LD 100 tris										X		X			X	X			
LD 100 bis															X	X			
LD 100 A															X				
LD 100						X										X			
LD 99															X				
LD 96, LD 97						X													
LD 95					X		X								X	X			
LD 94					X														
LD 92, LD 93													X			X			
LD 89				X															
Section H																			
LD 32																X			
LD 31															X	X			
LD 30				X	X	X									X	X			
LD 28					X										X		X		X
LD 27					X										X				X

Tab. 2 - Conodont distribution in the stratigraphic sections of Fig. 10 and 11.

A few representatives of *G. bulgarica* and *G. bifurcata hanbulogi* have been found at the base of the formation (section F, sample GL127) (Fig. 11, Tab. 2), suggesting Pelsonian-Illyrian age.

Adhami Limestone (Dercourt, 1964).

This formation, described for the first time by Renz (1906), is known in the literature also with the name of "Hornstein Plattenkalk". The name Adhami has been introduced by Dercourt (1964) and derives from a small village on the Argolis peninsula.

The Adhami Limestone consists of cm to dm-thick beds of limestone with chert nodules and bands. The thickness varies abruptly, ranging from 60 m in the northern thrust sheets to 200 m in the southern thrust sheet. In the latter, we have distinguished and mapped three members on the basis of lithologic differences:

- Adhami Limestone, lower member: cm-thick beds of chert with subordinate limestone levels. The thickness of this member varies from 5 to 30 m.

- Adhami Limestone, middle member: cm to dm-thick beds of limestone with chert nodules and lists. This member is the only one of the Adhami Lmst. that outcrops in the northern thrust sheets. The thickness varies from 50 to 200 m.

- Adhami Limestone, upper member: m-thick beds of limestone with few chert nodules. The thickness has been evaluated at 40 m.

The Adhami Limestone is usually bounded at the top by Jurassic Radiolarites, except in the area south of Hydra Chora where it is overlain by the Ammonitico Rosso. This last contact lies on top of a 80 cm-thick level of pinky matrix bearing breccias with limestone clasts and red chert bands. In both cases the presence of a hiatus at the contact has been inferred. Furthermore, the Adhami Lmst. is laterally limited by the Malies Facies of the Pantokrator Limestone.

Lithology and microfacies. - Adhami Lmst., lower member. It consists of cm-thick planar beds of red chert alternating with levels of red clay. Few gray to pink limestone beds with chert nodules and lists, laterally discontinuous, have also been detected. In the area west of Pr. Elias monastery, the lower member is made of cm-thick beds of green chert with rare green tuff levels.

- Adhami Lmst., middle member. It consists of centimetric to decimetric planar beds of filament-bearing gray limestone with chert in nodules and bands, sometimes very continuous. Centimetric levels of red clay and millimetric smearings of green tuff are also present. Approximately four metric levels of gray calcarenite without chert, interpreted as resedimented events coming from the Pantokrator platform, have also been detected, together with some slump structures. The microfacies of Adhami Lmst. chiefly consists of wackestones with radiolarians and filaments, frequently concentrated and oriented in accumulation levels. Conodonts and rare echinoderms are present.

- Adhami Lmst., upper member. It is composed of metre thick beds of gray limestone with few chert in irregular nodules and bands. The main microfacies consists of wackestones and packstones with unrecognizable particles of carbonate platform origin.

Age. The conodont fauna found in the Adhami Limestone is less abundant than in the previous formations and it mostly comes from the upper part (sections A, C, E) (Fig.10, 11; Tab. 2). It consists of *Gondolella polygnathiformis* (Budurov & Stefanov) (section E, GL118-119, H73; section A, GL50) with a few representatives of *Gondolella tadpole* Hayashi (section A, GL45, H29; section E, GL121). Some specimens of juvenile *Gondolella trammeri* (Early Ladinian) occur at the base (section C, H33).

The age of Adhami Limestone ranges from Early Ladinian (lower member) into Late Triassic. No conodonts were recovered from the upper member.

Depositional environment. The Adhami Lmst. was deposited in a pelagic environment. The Adhami Lmst., lower member, cropping out in the southern thrust sheet, probably represents the interval of time between the downwarping of the Eros platform and the rising of the Pantokrator platform. The lack and/or the distance of the "carbonate factory", probably associated with the Ladinian blooming of radiolarians promote a condensed siliceous sedimentation.

Later, the rising and growing of Pantokrator platform resulted in a rapid increase in micrite supply, leading to accumulation of the thick pelagic cherty limestone of the Adhami Lmst., middle member. Episodes of resedimentation of carbonate platform material affected the sedimentation of the upper part of the Adhami Lmst. Finally, the upper member of the Adhami Lmst. testifies to the redeposition of abundant material of platform origin.

As it is shown on the map, Adhami Lmst. crops out widely in the southern thrust sheet, whereas in the northern sheets the Malies facies of Pantokrator Lmst. is more widespread. This formation is very similar to Adhami Lmst. upper member, differing from it in being more proximal to the platform, thus more massive, coarsergrained and avoid of chert. If the synchroneity between the Adhami Lmst. and the Malies Facies of Pantokrator Lmst. is correctly interpreted, the latter represents very thick resedimentation in a deeper trough, which acted as a sediment trap (Fig. 13). Meanwhile the Adhami Lmst. initially developed in a pelagic environment away from the trough. Later, after the filling of the trough, the resedimented material of the Pantokrator platform entered the pelagic environment resulting in the deposition of the Adhami Lmst. upper member.

Pantokrator Limestone (Renz, 1906).

This formation consists of grey to dark grey limestones, rich in calcareous Algae, and foraminifers, with biohermal buildups associated with breccias and dark cements. It has been mapped by Römermann et al. (1981) with the name of Pantokra-
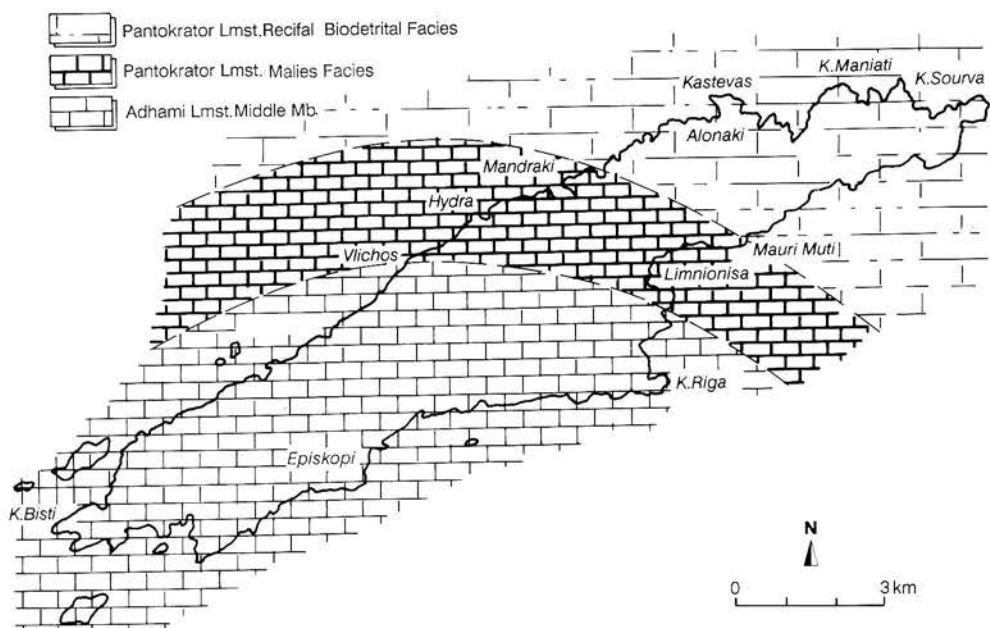
Fig. 13 - Palinspastic reconstruction during Ladinian.

tor Limestone and later it has been studied with the same name by Schäfer & Senow-bari-Daryan (1984). We accept the name Pantokrator even if it was proposed for the first time in the Ionian Zone by Renz (1906). In fact we do not want to overburden the stratigraphic nomenclature.

The Pantokrator Limestone is poorly bedded at the base, massive in the middle and well bedded at the top where desiccation features and dolomitic beds occur. The thickness reaches a maximum of more than 1100 m. This formation forms most of the Ompori thrust sheet.

Schäfer and Senowbari-Daryan (1984) distinguished only three, partially correlative lithofacies: biodetrital facies, recifal facies and loferitic facies into the Pantokrator Limestone. In this paper we introduce a new lithofacies, the Malies facies of Pantokrator Limestone.

Pantokrator Limestone, biodetrital facies.

This facies represents most of the base of the Pantokrator succession. It forms the south-eastern cliffs of Hydra and ranges from a thickness of 0 (at east of Hydra Chora) to 800 m (at east of O. Ompori). It is bounded at the top and partially synchronous with the recifal facies.

Lithology. This facies is represented by poorly bedded grey limestones with fibrous dark cements. Sorted levels are very scattered and tend to pinch out laterally.

Some of them show slightly erosive basal surfaces and pass vertically from mudstones to packstones/grainstones. Breccias are usually found with dark fibrous cements, easily detectable in the field. These breccias seem to increase towards the east and occur mainly near some small reef knolls containing corals, sponges and calcarous Algae. A bed with patch reef, breccias, cements and red sediment at its top, has been found on the top of O. Ompori.

Microfacies. Grainstones and packstones are predominant with minor wackestones and mudstones. It is possible to recognize (in order of abundance): limestone clasts, pellets, oncoids/oncolites, filaments, calcareous Algae (nodular, erect and encrusting forms) some of them still in a living position forming bafflestones, foraminifers, corals, sponges, *incertae sedis*. The floral association is represented by encrusting forms such as *Spongiostromata* sensu Pia and *Tubiphytes obscurus*, with little "bushy" forms (few mm) of *Cayeuxia* sp. and *Cladogirvanella cipitensis* Ott. Minor forms are: *Bacinella ordinata* Pantic, *Microtubus communis* Flügel, *Tubiphytes carinthiacus*, *Poriferitubus buseri*, *Cyanophyta* sp., *Porostromata* sp., *Sphaerocodium* sp., *Orthonella* sp. and dasyclad fragments. Foraminifers include: *Pilamminella semiplana* (Kochansky-Devidé & Pantic), *Planiinvoluta* sp., *Planiinvoluta carinata* Leischner, *Ophthalmidium martanum* (Farinacci), *Ophthalmidium* sp., *Pseudoglandulina conica* Miklucho-Maklay, *Reophax* sp., *Tolypammina* sp., *Pseudobolivina globosa* Kristan-Tollmann, *Quinqueloculina* sp., *Turrispirillina* sp., *Turrispirillina prealpina* Zaninetti & Brönnimann, *Meandrospira* sp. and *Duostominidae*.

Age. The age of the biodetrital facies of the Pantokrator Lmst. probably ranges from Late Anisian/Early Ladinian (Han Bulog topmost part with conodonts; Fig.10, 11), to Carnian or Carnian/Norian, based on the foraminifer association.

Depositional environment. This facies may represent a slightly lower area during the early stage of the platform growth. In fact sediments coming from the partial disruption of the western reef margin deposited in this lower area, as testified by the outcrops near Hydra Chora. This picture is consistent with the extreme fragmentation and composition of the sediments. The presence of scattered small patch reefs may indicate some differences in the topography of the area which can be considered as an inner part of the platform. The depth locally varied but did not exceed a few tens of metres as witnessed by the O. Ompori emersion surface.

Pantokrator Limestone recifal facies.

Its mean thickness is of 180/200 m, reaching a maximum of 300 m between O. Ompori and Mandraki. It is bounded at the top by the loferitic facies. The boundary is represented by an increased bedding and by the appearance of dolomites with few red cements at the top of the last patch reef (e.g. Megale Vigla). Elsewhere (e.g. Kastevas) about 10 m of grey grainstones and packstones with few mudstones, rich in coral and sponge fragments have been detected.

Lithology. The recifal facies is particularly well exposed near Mandraki. It consists of buildups (patch reefs) (Fig. 14), breccias (mainly talus) and large areas with

dark cements (Fig. 15). The latter is the most striking feature where patch reefs are not evident. Red cements within the reefs and their talus are locally present. This facies shows two different types of development: 1) the reef developed along the whole outcrop thickness (i.e. near Mandraki and in the western area); and 2) patch reefs tend to be more and more scattered and small. In this last case breccias and algal bafflestones become predominant.

Microfacies. The microfacies consists of boundstones and bioclastic packstones and wackestones with graded matrix. Commonly corals and sponges are heavily recrystallized (sparry calcite) and are encrusted by epibionts (Algae and foraminifers). Calcareous Algae may have helped to stabilizing and trapping the sediment. Foraminifers are common in the granular fraction.

The paleontological content of this facies includes: corals (cf. "*Thecosmilia*" and very low thammasteroids colonies), mostly recrystallized sponges (*Cryptocoelia* cf. *zitteli* Steinmann, *Uvanella irregularis* Ott, *Cryptocoelia* sp.). Furthermore *Cladogirvanella cipitensis*, *Girvanella* sp., *Orthonella* sp., *Cayeuxia* sp., *Solenopora* sp., *Spongiostromata* sensu Pia, *Tubiphytes obscurus*, *T. carynthiacus*, *Thaumatoporella* cf. *parvovesiculifera* Raineri, *Thaumatoporella* sp., *Baccanella floriformis*, *Macrotubus babai* Fois; *Microtubus communis* and dasycladaceans (*Aciculella* sp.) have been detected.

Foraminifers include: *Angulodiscus parallelus* (Kristan-Tollmann), *Meandrospira deformata*, *Planiinvoluta regularis* Salaj, Samuel & Borza, *Permodiscus planidiscoides* Oberhauser, *Sigmoilina multicarinata* Salaj, Samuel & Borza, *Pseudocucurbita campanuliformis* Borza & Samuel, *Haplophragmella irregularis* (Rauser-Chernousova), *Tetrataxis inflata*, *Angulodiscus communis* Kristan, *A. friedli* (Kristan-Tollmann), *Variostoma catilliforme* Kristan-Tollmann, *Agathammina austroalpina*, *Nodosaria* sp., *Planiinvoluta* sp., *Endothyranella* sp., *Tolypammina* sp., *Ophthalmidiidae*, *Duostominidae* and *Miliolidae*.

Age. The foraminifer association indicates a Carnian-Norian age. Since this facies overlies Han Bulog Lmst. near Hydra Chora, it therefore ranges from the Late Anisian/Early Ladinian up to Norian.

Depositional environment. During the reef stage, the topography of the Pantokrator platform was characterized by higher areas, where the reef was already present and lower areas, where talus breccias and highly fragmented sediments were deposited. Moreover, it is possible to locate an inner and quieter area towards the south-east, witnessed by fewer and smaller patch reefs and by the presence of *Uvanella irregularis*. Towards north-west a well developed reef and highly disrupted dasycladacean Algae seem to indicate higher energy. During this stage, a few emersions may occur as witnessed by red cements found inside some coral.

Pantokrator Limestone, Ioferitic facies.

This facies outcrops in the north-eastern part of the island, from west of Kap Kastevas to the promontory between Kap Bretista and Kap Maniati. It is 230 m thick

Fig. 14 - Photo of corals in life position in the recifal facies of Pantokrator Lmst. near Hydra Chora.

Fig. 15 - Breccias with cements in the recifal facies of Pantokrator Lmst.

and its upper boundary is only exposed at Kap Kastevas, where it is overlain by Ammonitico Rosso.

Lithology and microfacies. The most peculiar feature of this well bedded facies, is its marked cyclicity. The facies consists of grey to light grey limestones, mudstones to grainstones, associated with milky white dolomites. It shows sheet and prism cracks, shrinkage pores often with carbonates solution and calcite precipitates such as fibrous cements. This facies has been divided into three lithozones:

- at the base dolomites are less common and algal laminae with debris and grain flows are quite frequent. The sediment is stabilized by encrusting blue-green Algae (*Spongiostromata*). This first lithozone shows only small shrinkage pores and represents a fining upward trend.

Fig. 16 - Cycles in the loferitic facies of Pantokrator Lmst. Each cycle is represented by basal grainstone and upper dolomitic level (white part in the photo).

- In the second lithozone (the thickest), cycles are much more evident. In each of them, from bottom to top, it is possible to recognize: basal grainstones with dolomite chips and abundant foraminifers and erect Algae (*Porostromata*); mudstones and wackestones with broken valves and few foraminifers; slightly bedded packstones and grainstones with intraclasts and *Spongiostromata* either in micritic matrix or in sparry calcite; dolomitic packstones and grainstones mainly with grapestones, algal tubes and fragments often with a red sediment filling. Sparry calcite is dominant. In this part of the cycle stromatolites are well developed and evident. The dolomitic uppermost part is usually slightly eroded by the basal grainstones of the following cycle (Fig. 16). The cycles are thicker (6/7 metres) at the base of the lithozone, whereas they hardly reach 1 metre at the top.

- The third lithozone is represented by fine grained limestones with banks very rich in gastropods and big megalodontids, passing upwards to reddish microbreccias with filaments. At Kap Kastevas a couple of metres of black mudstones with laminae and synsedimentary en-échelon microfaults, have been found. In thin sections they show small ostracod shells and stromatolites. The bioclasts of this lithozone include gastropods, bivalves, crinoids, ostracods, foraminifers and calcareous Algae. The last two groups are very well represented. Among foraminifers there are: *Angulodiscus friedli*, *Aulotortus sinuosus* Weynschenk, *Angulodiscus communis*, *Involutina sinuosa* (Weynschenk), *I. minuta* Koehn-Zaninetti, *Agathammina inconstans* Michalik, Jendresakova & Borza, *Variostoma cochlea* Kristan-Tollmann, *V. catilliforme*, *Tetrataxis nana*, *Ophthalmidium carinatum* (Leischner), *Semiinvoluta clari* Kristan and *Duostominidae*. Among problematica there are: *Microtubus* sp., *Macrotubus* sp., *Tubiphytes obscurus* and *T. carinthiacus* and among the Algae *Cayeuxia* sp. and *Orthonella* sp. have been detected.

Age. The age, according to the foraminifer association, should be Late Norian-Rhaetian. Moreover Salaj et al. (1983) consider the association of *Angulodiscus friedli-Semiinvoluta clari* as typical for the beds near the Norian/Rhaetian boundary.

Depositional environment. The loferitic facies represents, starting from its bottom and up to the second lithozone, a shallowing upward trend ending with an intertidal environment with frequent emersions. The third lithozone already marks the death of the whole carbonate platform with an increase in water depth. During the "loferitic" stage the Pantokrator platform appears to have lost its local irregularities developed during the reef stage. Nevertheless, as clearly shown by the black mudstones at Kap Kastevas, a few sub-environments could develope.

Pantokrator Limestone, Malies facies.

The Malies facies is here proposed to identify 80 to 150 m-thick grey massive limestones arranged in wide lenticular bodies. It was mapped in our geological map as resedimented Malies facies, but according to the international nomenclature, we establish the name Malies facies.

This lithofacies constitutes the backbone of O. Malies (from which its name derives) and crops out along the northern coast, westward of Hydra Chora (see our geological map).

The Malies facies of Pantokrator Limestone is unconformably overlain by Radiolarites. Although in the field this boundary might seem gradual, the presence of Ammonitico Rosso Lmst. elsewhere in the island makes more likely that a conspicuous hyatus divides these two formations. Laterally this facies gradually leads to the Adhami Lmst.

Lithology. At the base, the Malies facies consists of reef debris-bearing breccias with red matrix, passing vertically into a finer sediment, still grey, with centimetric clasts derived from the Pantokrator carbonate platform. At the top graded grainstones and packstones occur associated with thin pinkish to reddish levels (1 to 10 cm-s thick).

Microfacies. The main microfacies is represented by packstones, grainstones and microbreccias with bioclasts, peloids and ooids. Among the bioclasts there are echinoderms, bivalves, corals, gastropods, sponges (*Cryptocoelia* sp.), Algae (*Cayeuxia* sp., *Orthonella* sp. and dasycladaceans), problematica (*Tubiphytes obscurus, T. carinthiacus, Archaeolithoporella* sp., *Baccanella floriformis, Bacinella irregularis, Microtubus communis, Microtubus* sp.) and foraminifers [*Endothyranella* sp., *Nodosaria ordinata* Trifonova, *Variostoma catilliforme* Kristan-Tollmann, *Angulodiscus* sp., *Aulotortus* sp., *Sigmoilina bystrickyi* Salay, Borza & Samuel, *Sigmoilina* sp., *Ophthalmidium* sp., *Planiinvoluta* sp., *P. irregularis* Salaj, Samuel & Borza, *Palaeomiliolina* sp., *Urnulinella andrusovi* Borza & Samuel, *Tetrataxis* sp., *Auloconus permodiscoides* (Oberhauser), *Quinqueloculina* sp., *Meandrospira* sp., *Duostominidae*, rare *Triasina* sp. and very abundant *Galeanella panticae* Zaninetti & Brönnimann and *Galeanella tollmanni* (Kristan)].

At O. Malies samples coming from the boundary with Radiolarites consist of mudstone with filaments and radiolarians and of microbreccias with centimetric Pantokrator Lmst. clasts in a red matrix also containing filaments and radiolarians.

Age. In the westernmost part of the island, the Malies facies of the Pantokrator Lmst., overlies a few metres of Adhami Lmst. with Carnian conodonts (sect. E) (Fig. 11, Tab. 2).

In the area west of Vlichos the base of Malies facies occupies the lowest stratigraphic position lying on top of the transitional facies with the Han Bulog Lmst., which contains an Illyrian conodont association (sect. B) (Fig. 11, Tab. 2).

At O. Malies the foraminifer association suggests a Norian-Raethian age. In particular the occurrence of *Galeanella panticae, G. tollmanni* and *Triasina* sp. in the upper levels of this facies indicates a latest Triassic age according to Trifonova (1980).

Depositional environment. The wide lenticular bodies of the Malies facies represent episodes of resedimentation of Pantokrator Lmst. material in a deeper and southern area, whilst towards north the loferitic facies kept developing. In the more distal areas the Malies facies passes into Adhami Lmst. which is poorer in resedimented carbonates and richer in silica.

Jurassic formations.

Hydra's sedimentary succession comprises two Jurassic formations: Ammonitico Rosso and Radiolarites, both presently studied by P. Baumgartner, Lausanne. Since the aim of our work was to study the Triassic, we only provide some new information on the micropaleontological content (i.e. foraminifers and coccoliths) and areal distribution of the two Jurassic formations stated by Römermann (1968). Furthermore we signal the occurrence of olistoliths in the Radiolarites for the first time.

The relationships between the Triassic and the Jurassic formations are depicted in Fig. 17.

Ammonitico Rosso Limestone (Römermann, 1968).

This formation attains its maximum thickness of 30 m at Kap Kastevas. The few other outcrops in the island barely reach 3 m. At Kap Kastevas the passage between Ammonitico Rosso Lmst. and the overlying Radiolarites seems to be sharp and possibly slightly affected by tectonics. Indeed polygenic breccias in a red matrix pass abruptly to a siliceous brownish sediment with few carbonates and marls in 1 to 10 cm-thick levels.

Lithology and microfacies. Ammonitico Rosso Lmst. is composed mainly of red and grey highly nodular limestones becoming more and more rich in terrigenous sediment and Fe-oxides towards the top.

Thin sections show a gradual change in clasts composition: at the base they mainly consist of platform particles (i.e. foraminifers, gastropods, Algae), while towards the top, filaments, little ammonoids and a different foraminifers association characterize the silty red matrix of the breccias. Foraminifers are very often strongly micritized or recrystallized and include *Involutina liassica* (Jones), *I. turgida* Kristan, *I. communis* (Kristan), *Frondicularia xiphoidea* Kristan-Tollmann, *Planiinvoluta carinata* Leishner, *Nodosaria nitida elongata* Franke, *Nodosaria* sp., *Lingulina tenera* Born, *Vidalina* sp., *Pseudonodosaria* sp., *Lenticulina* sp., *Lagenidae*. Very often foraminifers are the nucleus of oncoids which are the only algal material in the Ammonitico Rosso. Gastropods, ammonites, filaments, ostracods, echinoids and radiolarians which tend to increase towards the top are also present. Because of the pervasive sparry only one coccolite form could be determined: *Schizosphaerella punctulata* Deflandre & Dangeart (which spans from Early Hettangian to the Late Oxfordian).

Age. According to the paleontological record in Römermann (1968) [*Lytoceras fimbriatum* (Sowerby), *Audaxlytoceras audax* (Meneghini), *Audaxlytoceras* sp. ex aff. *A. audax* (Meneghini), *Zetoceras* sp. ex aff. *Z. bonarellii* (Bettoni)] and to the foraminifers listed above Ammonitico Rosso Lmst. is Early Jurassic in age, possibly spanning the Hettangian and Sinemurian time interval.

Depositional environment. Ammonitico Rosso Lmst. clearly represents the drowning of the Pantokrator platform probably due to the widespread Jurassic trans-

gression. Benthos and bioturbation indicate a quiet and well oxygenated bottom. Upward the nodularity increases showing a lower sedimentation rate; these conditions seem to be typical of a pelagic plateau. At the top, large breccias testify a major tectonic activity after which a deeper siliceous deposition starts.
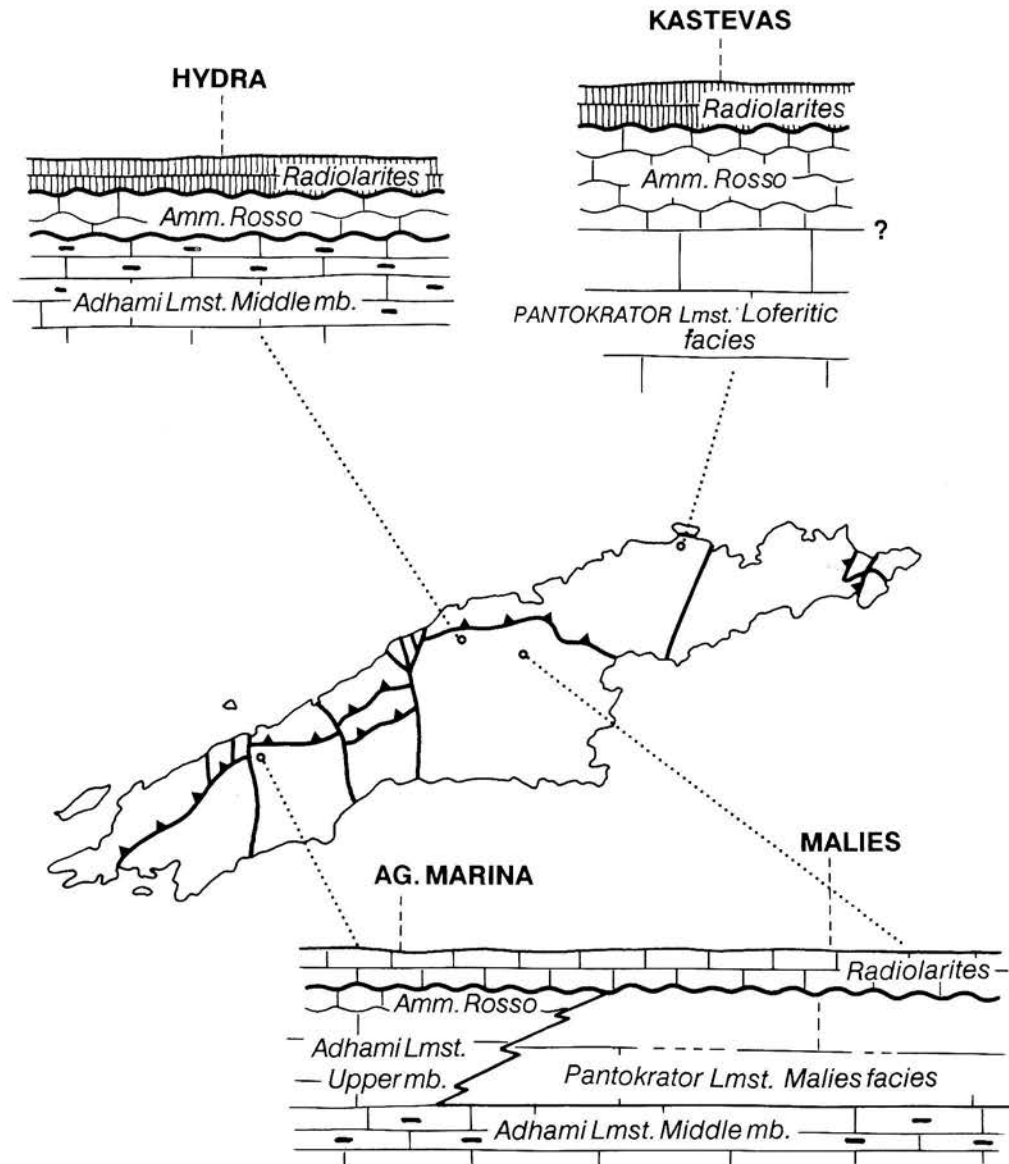
Fig. 17 - Stratigraphy of the Triassic-Jurassic boundary: synthetic representation of three situations encountered. See text for the description of the formations.

Radiolarites Formation (Römermann, 1968).

Radiolarites Fm. crops out at the top of the stratigraphic succession of Hydra. Due to the presence of tectonic lineaments or of the sea, it is impossible to describe upper boundary or estimate its thickness.

Lithology. It is composed chiefly of a silty and sometimes marly brownish red siliceous sediment. Radiolarites Fm. has been divided into two members. In the first member olistoliths have been found (Olistolith Member). They show different sizes and composition being related to Adhami, Pantokrator and Eros formations. They all are deeply recrystallized. The second member crops out at Kap Kastevas (Kastevas Member) where radiolarites show coarser grains and texture, more carbonates and few light blue/green cherty levels.

Microfacies and age. Besides radiolarians, two coccolites have been found: *Watznaueria* sp. and *Schizosphaerella punctulata.* According to their concurrent age (Aalenian-Oxfordian), it is possible that deposition of the Hydra's Radiolarites started slightly before those of Argolis, sometimes between the Aalenian and Oxfordian.

Depositional environment. The Radiolarites Fm. of Hydra recorded the deepening of the Adhami Lmst. and Ammonitico Rosso Lmst. basins. It is wise to consider that the Kastevas Member, richer in carbonates, could represent a higher environment than the Olistolith Member. The latter seems to be contemporaneous with the inception of compressive tectonic activity (accretionary prism ?) during Jurassic as suggested by the presence of a large number of Triassic rock-bearing olistoliths.

Paleoenvironmental evolution

Hydra sedimentary succession records the typical evolution of a passive continental margin. During Permian three main carbonate platforms developed, separated by terrigenous events, chiefly consisting of arkoses.

The base of the Triassic succession consists of quartzarenites. Subsequently, during Late Scythian-Early Anisian a progressive increase in carbonate supply, coupled with a high rate of subsidence, produced a very thick carbonate platform (Eros Lmst.). During Pelsonian, in the central-western part of Hydra the rate of subsidence was no more balanced by the carbonate supply and a pelagic succession developed (Han Bulog and Adhami Lmsts.). In the eastern part, a carbonate platform (Pantokrator Lmst.) grew from Ladinian to Late Triassic, the carbonate supply balancing the very high rate of subsidence.

Widespread pelagic conditions are set up during Jurassic with the deposition of red nodular limestone and red chert (Ammonitico Rosso and Radiolarites Fms.).

Geodynamic interpretation

The stratigraphic succession of the island of Hydra can be subdivided into three main supercycles:

A) *Permian*. It is represented by two major transgressive-regressive cycles, the older starting with the sandstone and conglomerate of the Nisisa Fm. (stratigraphic terminology after Baud et al., 1991) and continuing with the limestone of the Thikia Gr. p.p., whereas the second, immediately succeeding, starts with the siltstone of Kap Bisti Gr. p.p. and carries on with the limestone of the Episkopi Fm. The Late Permian Miras Fm. represents a minor erosional episode which locally dissects the top of Episkopi Fm. and is clearly distinct from the Ag. Nikolaos Fm. which marks the beginning of the Triassic sequence. According to our interpretation these pulses are related to extensional tectonic with block-faulting, tilting and erosion. Baud et al. (1991) distinguish four events in the sedimentary succession consisting of the Permian groups plus the Eros Lmst. of Hydra and relate them to the closure of Paleotethys.

In any case there is a fairly good agreement with the Lower Permian succession of Carnia and Karavanke, testifying that Hydra had a similar evolution during this period. Later, the Episkopi and Miras Fms. quite differ from Bellerophon Fm.

B) *Triassic*. Late Scythian-Early Anisian is characterized by the rising and growing of the carbonate platform of Eros Lmst. Its downwarping, dated as Early Pelsonian, marks the beginning of a period of very high subsidence, represented by the progressively deeper facies overlying Eros Lmst., continuing through most of the Jurassic. This deepening is interpreted as related to a continental rifting phase, followed by the drifting of the Pelagonian microplate away from the Gondwana margin. Tectonic activity is also witnessed by the presence of Quarz keratophyric tuffs. In the eastern part of the island, where very high rates of subsidence were balanced by the carbonate sedimentation, the carbonate platform represented by the Pantokrator Lmst. developed from Ladinian to Late Triassic.

C) *Jurassic*. This system records a drastic drop in rate of sedimentation. Few metres of Ammonitico Rosso Lmst. and of Radiolarites Fm., bounded by important hiatuses, constitute the sequence. Radiolarite through plays an important geodynamic role, hosting a great number of olistoliths of Triassic rocks, probably related to a compressive tectonic activity. According to Mountrakis et al. (1987) the Internal Hellenides Mountain Range started to stack during Late Jurassic-Early Cretaceous time.

On these considerations, the Triassic to Jurassic sequence of the island of Hydra has recorded the development of a passive continental margin succession, the geologic history of which is depicted in Fig. 18. The concept of Subpelagonian zone proposed by Jacobshagen (1977, 1989 pers. comm.), i.e. a NW-SE isopic zone characterized by a passive continental margin succession striking parallel to the Pelagonian Microplate, is in agreement with our analysis. The Middle Triassic rifting phase recorded in the
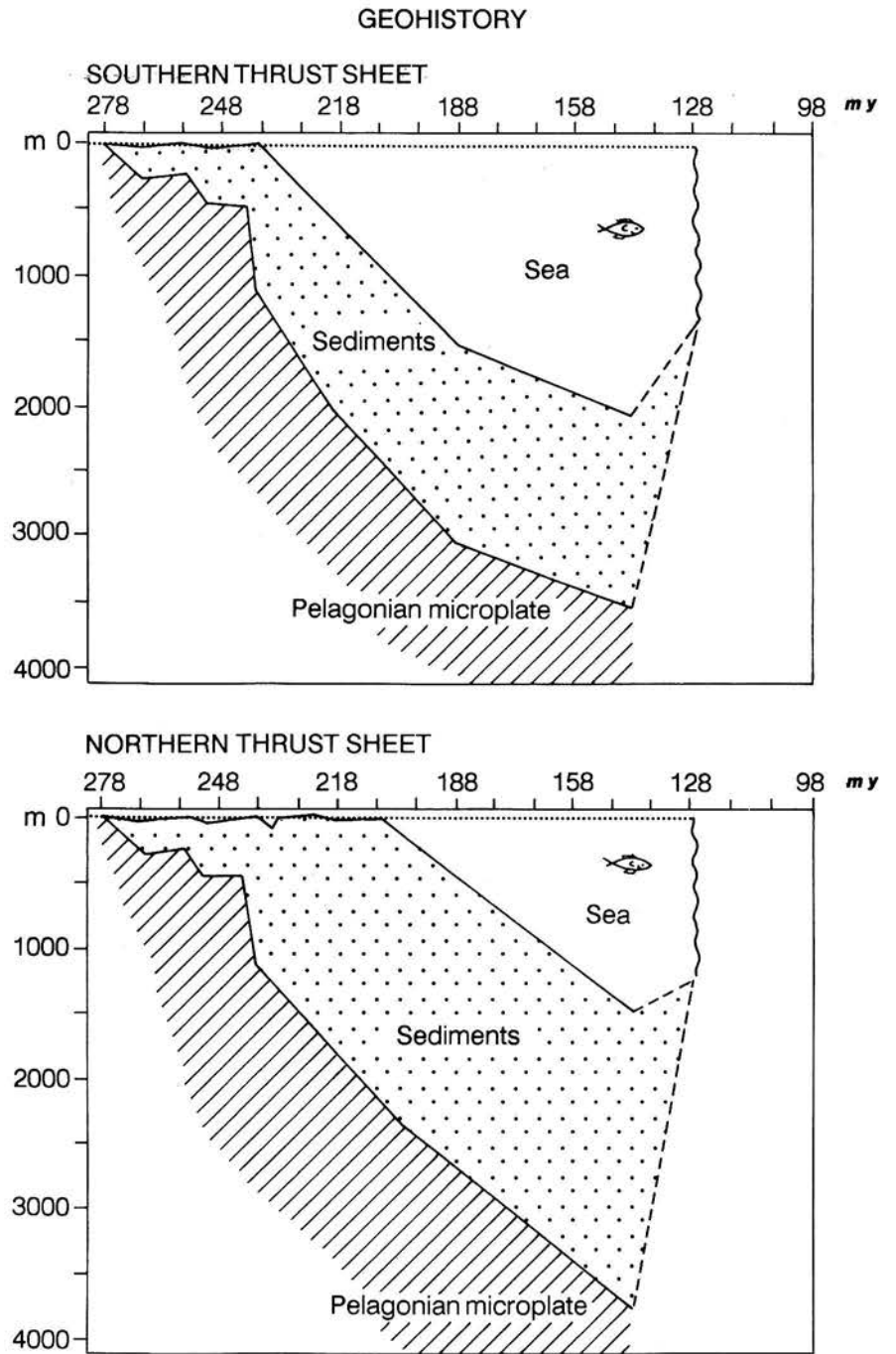
GEOHISTORY

Fig. 18 - Geohistory of the Paleozoic and Mesozoic succession of Hydra Island. See text for discussion.

rocks of Hydra is linked to the identification of the Pelagonian Microplate. The olistoliths inbedded in the Radiolarites seem to suggest that the Middle Triassic-Jurassic deep basin underwent transpressive (or simply compressive) movements during Late Jurassic.

REFERENCES

Bannert D. & Bender H. (1968) - Zur Geologie der Argolis-Halbinsel (Peloponnes, Griechenland). *Geol. Palaeont.*, n. 2, pp. 151-162, Marburg.

Baud A., Jenny C., Papanikolaou D., Sideris Ch. & Stampfli G. (1991) - New observations on Permian stratigraphy in Greece and geodynamic interpretation. *Bull. Geol. Soc. Greece*, v. 25, n. 1, pp. 187-206, Athens.

Baumgartner P.O. (1985) - Jurassic sedimentary evolution and nappe emplacement in the Argolis peninsula. *Denkschr. Schweiz. Naturforsch. Gesell.*, v. 99, 111 pp., Basel.

Bender H., Hirschberg K., Leuteritz K. & Mänz H. (1960) - Zur Geologie der Olonos-Pindos und der Parnass-Kiona-Zone im Tale des Asklepieion (Argolis). *Ann. Géol. Pays Hellén.*, n. 11, pp. 201-213, Athens.

Channel J.E.T. & Horvath F. (1976) - The African/Adriatic promontory as a paleogeographical premise for alpine orogeny and plate movements in the Carpatho-Balkan region. *Tectonophysics*, v. 35, pp. 71-101, Amsterdam.

Dercourt J. (1964) - Contribution à l'étude géologique d'un secteur du Péloponnèse septentrionale. *Ann. Géol. Pays Hellén.*, n. 15, pp. 1-417, Athens.

Dixon J.E. & Robertson A.H.F. (1984) - The geological evolution of the eastern Mediterranean. *Geol. Soc., Spec. Publ.*, n. 17, 824 pp., Oxford.

Durkoop A., Richter D.K. & Stritzche R. (1986) - Fazies, Alter und Korrelation der triadischen Rotkalke von Epidaurus, Adhami und Hydra (Griechenland). *Facies*, n. 14, pp. 105-150, Erlangen.

Grant R.E. (1972) - The lophophore and feeding mechanism of Productidina (Brachiopoda). *Journ. Paleont.*, v. 46, n. 2, pp. 213-249, Tulsa.

Grant R.E., Nestell M.K., Baud A. & Jenny C. (1991) - Permian Stratigraphy of Hydra Island, Greece. *Palaios*, v. 6, pp. 479-497, Tulsa.

Haralambous D. (1963) - Ein Profil vom Karbon bis zur Trias auf Hydra (Griechenland). *Bull. Geol. Soc. Greece*, v. 5, pp. 20-28, Athens.

Harland W.B., Armstrong R.L., Cox A.V., Craig L.E., Smith A.G. & Smith D.G. (1990) - A geologic time scale 1989. Cambridge Univ. Press, pp. 1-263, Cambridge.

Hauer F.v. (1884) - Cephalopoden der unteren Trias vom Han Bulog an der Miliaka OSO von Sarajewo. *Verh. Geol. Reichsanst.*, v. 1884, pp. 217-219, Wien.

Jacobshagen V. (1986) - Geologie von Griechenland. V. of 363 pp., Berlin.

Jacobshagen V., Martz J. & Reinhardt R. (1977) - Eine alttertiare Ophiolith-Decke in den inneren Helleniden NE-Griechenlands. *N. Jb. Geol. Paläont.*, n. 1977, pp. 613-620, Stuttgart.

Leven E. Y. (1981) - Permian Tethys Stage Scale and correlation of sections of the Mediterranean-Alpine folded belt. *IGCP n. 5, Newsletter*, v. 3, Karamata S. & Sassi F.P. (Eds.), pp. 100-112, Padova.

Milch L. & Renz C. (1911) - Über griechische Quarzkeratophyre. *N. Jb. Mineral.*, v. 31, pp. 496-534, Stuttgart.

Mountrakis D., Patras D., Kilias A., Pavlides S. & Spyropoulos N. (1987) - Structural geology of the Internal Hellenides and their role to the geotectonic evolution of the eastern Mediterranean. *Acta Natur. Ateneo Parmense*, n. 23, pp. 147-162, Parma.

Nestell M.K. & Wardlaw B.R. (1987) - Upper Permian Conodonts from Hydra, Greece. *Journ. Paleont.*, v. 61, n. 4, pp. 758-772, Tulsa.

Okonomidis G. Th. (1940) - Beiträge zur Geologie der ostpeloponnesischen Kuste (Insel Hydra v. Kynuria). *Zeitschr. Bulgar. Geol. Ges.*, v. 11., pp. 67-80, Sofia.

Oravecz-Scheffer A. (1987) - Triassic foraminifers of the Transdanubian central range. *Geol. Hungarica*, n. 50, 331 pp., Budapest.

Philippson A. (1892) - Der Peloponnes. Versuch einer Landeskunde auf geologischer Grundlage, 642 pp., Berlin.

Renz C. (1906) - Trias und Jura in der Argolis. *Zeitschr. Deut. Geol. Ges.*, v. 58, pp. 379-395, Berlin.

Renz C. (1910) - Stratigraphische Untersuchungen im griechischen Mesozoikum und Paläozoikum. *Jahrb. K. K. Geol. Reichsanst.*, v. 60, pp. 421-636, Wien.

Renz C. (1925) - Zur Geologie der Insel Hydra. *Ecl. Geol. Helv.*, v. 19, pp. 363-372, Basel.

Renz C. (1931) - Die Bulogkalke der Insel Hydra (Ostpeloponnes). *Ecl. Geol. Helv.*, v. 24, pp. 53-60, Basel.

Renz C. (1955) - Die Vorneogene Stratigraphie der normalsedimentaren Formationen Griechenlands. *Inst. Geol. Subsurf. Res.*, 637 pp., Athens.

Richter D.K. & Fuchtbauer H. (1981) - Merkmale und Genese von Breccen und ihre Bedeutung im Mesozoikum von Hydra. *Zeitschr. Deut. Geol. Ges.*, v. 132, pp. 451-50, Hannover.

Römermann H. (1968) - Geologie von Hydra (Griechenland). *Geol. Palaeont.*, v. 2, pp. 163-171, Marburg.

Römermann H., Graf W., Huckriede P., Jacobshagen V., Kahler F., Walliser H., Zapfe H., & Bornovas J. (1981) - Hydra: In the collection Geological Maps 1:50000. *Geol. Surv. Greece*, I.G.M.E., Athens.

Salaj J., Borza K. & Samuel O. (1983) - Triassic Foraminifers of the west Carpathians. V. of 213 pp., Bratislava.

Schäfer P. & Senowbari-Daryan M. (1984) - The Upper Triassic Pantokrator Limestone of Hydra, Greece: An Example of a Prograding Reef Complex. *Facies*, n. 6, pp.147-164, Erlangen.

Trifonova E. (1980) - On the foraminifera microbiofacies in the Triassic from N Bulgaria. *Riv. It. Paleont. Strat.*, v. 85, n. 3-4, pp. 781-788, Milano.

Wendt J. (1973) - Cephalopod accumulations in the Middle Triassic Hallstatt-Limestone of Jugoslavia and Greece. *N. Jb. Geol. Paläont.*, v. 28, n. 4, pp. 624-640, Stuttgart.

PLATE 12

Fig. 1 - Eros Lmst., lower lithozone. Oolitic grainstone with detrital quartz. GL 168 (O. Zakoni); X 8.

Fig. 2 - Eros Lmst., lower lithozone. Oolitic grainstone with quartz grains. GL 83 (O. Zakoni); X 4.

Fig. 3 - Eros Lmst., lower lithozone. Oolitic grainstone with gastropods. GL 302 (Episkopi); X 6.

Fig. 4 - Eros Lmst., lower lithozone. Oolitic grainstone with intraclasts. GL 302 (Episkopi); X 6.

Fig. 5 - Eros Lmst. s.s., microfacies B3. *Palaeomiliolina judicariensis?* (Premoli Silva). GL346 (Ag. Marina); X 30.

Fig. 6 - Eros Lmst. s.s., microfacies C4. *Duostominidae.* GL 59 (O. Purgos section); X 16.

Fig. 7 - Han Bulog Lmst. Filament and subordinate radiolarian accumulation level with stylolite. LD 31 (Aghios Triados); X 10.

Fig. 8 - Pantokrator Lmst., recifal facies. Coral bafflestone. A) *Cayeuxia* sp.; B) *Tolypammina* sp.; C) encrusting blue/green Algae. LD 64B (Koku); X 6.

Fig. 9 - Pantokrator Lmst., loferitic facies. Synsedimentary fracture in sorted deposit. LD 74 (Kastevas); X 2.5.

Fig. 10 - Pantokrator Lmst., Malies facies. *Galeanella panticae* Zaninetti & Brönnimann. LD 9 (O. Malies); X 20.

PLATE 13

Fig. 1 - *Hindeodus julfensis* (Sweet). Lateral wiew. Miras Fm. Sample H141 (600 m west of Gherakina); X 50.

Fig. 2 - *Neospathodus homeri* (Bender). Eros Lmst. s.s. Sample MR225 (O. Zakoni). b, c; X 75.

Fig. 3 - *Gondolella bulgarica* (Budurov & Stefanov). Eros Lmst., upper lithozone. Section C, sample GL86. b, c; X 50.

Fig. 4 - *Gondolella bulgarica* (Budurov & Stefanov). Eros Lmst., upper lithozone. Section C, sample GL87. a, b; X 65.

Fig. 5 - *Neospathodus kockeli* (Tatge). Han Bulog Lmst. Section C, sample GL94; X 75.

Fig. 6 - Transitional form between *Gondolella bifurcata bifurcata* (Budurov & Stefanov) and *Gondolella bifurcata hanbulogi* (Sudar & Budurov). Eros Lmst., upper lithozone. Section C, sample GL91. a, b; X 50.

Fig. 7 - *Gondolella excelsa* (Mosher). Han Bulog Lmst. Section G, sample LD95. a, b; X 50, c; X 60.

Fig. 8 - *Gondolella excelsa* (Mosher). Eros Lmst., upper lithozone. Section C, sample GL91. a, b; X 40.

Fig. 9 - *Gondolella bifurcata hanbulogi* (Sudar & Budurov) juvenile specimen. Han Bulog Lmst. Section C, sample GL94; X 75.

Fig. 10 - *Gondolella bifurcata hanbulogi* (Sudar & Budurov) juvenile specimen. Han Bulog Lmst. Section C, sample GL94. b, c; X 75.

Fig. 11 - Transitional form between *Gondolella bifurcata bifurcata* (Budurov & Stefanov) and *Gondolella bifurcata hanbulogi* (Sudar & Budurov). Han Bulog Lmst. Section C, sample GL93. b, c; X 65.

Fig. 12 - *Gondolella bifurcata hanbulogi* (Sudar & Budurov). Han Bulog Lmst. Section C, sample GL97. a, b; X 50.

Fig. 13 - *Gondolella bifurcata hanbulogi* (Sudar & Budurov). Han Bulog Lmst. Section C, sample GL97. a, b, c; X 50.

a) Upper view;
b) lateral view;
c) lower view.

PLATE 14

Fig. 1 - *Gondolella trammeri* Kozur. Han Bulog Lmst. Section C, sample H33. a, b, c; X 100.
Fig. 2 - *Gondolella* aff. *eotrammeri* Krystyn. Han Bulog Lmst. Section G, sample LD95. a, b, c; X 75.
Fig. 3 - Transitional form between *Gondolella foliata inclinata* Kovacs and *Gondolella polygnathiformis* (Budurov & Stefanov). Adhami Lmst. Section E, sample GL118. a, b; X 75.
Fig. 4 - *Gondolella* aff. *eotrammeri* Krystyn. Han Bulog Lmst. Section G, sample LD100. a, b, c; X 75.
Fig. 5 - *Gondolella polygnathiformis* (Budurov & Stefanov). Adhami Lmst. Section E, sample H73; X 100.
Fig. 6 - *Gondolella tadpole* Hayashi. Adhami Lmst. Section A, sample H29. b, d; X 75.
Fig. 7 - *Gondolella tadpole* Hayashi. Adhami Lmst. Section A, sample GL45. d, c; X 75.

a) Upper view;
b) lateral view;
c) lower view;
d) oblique/lateral view.
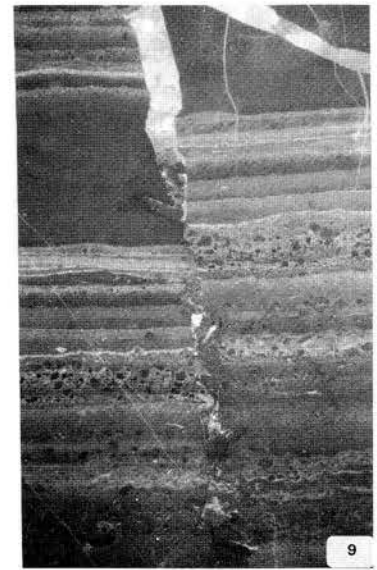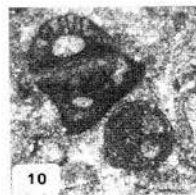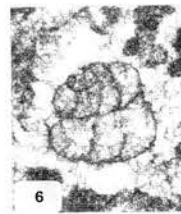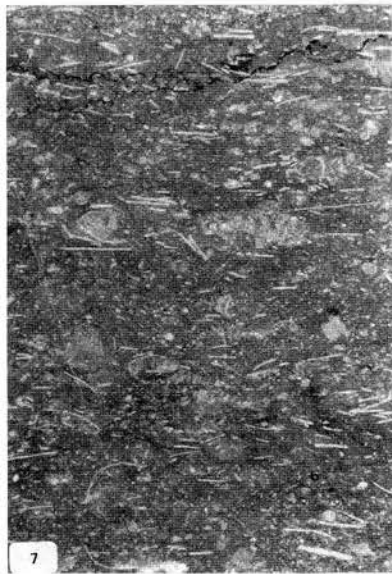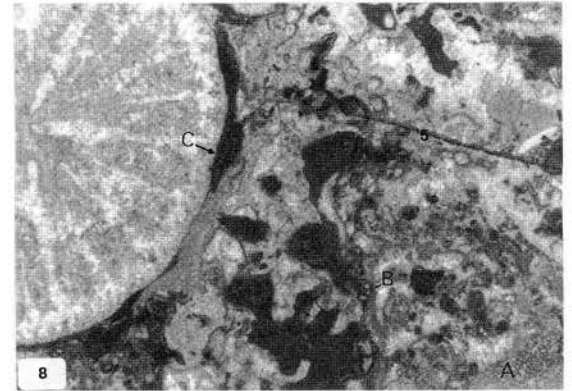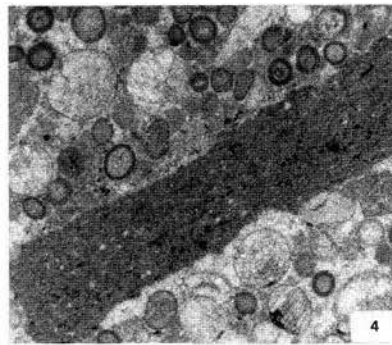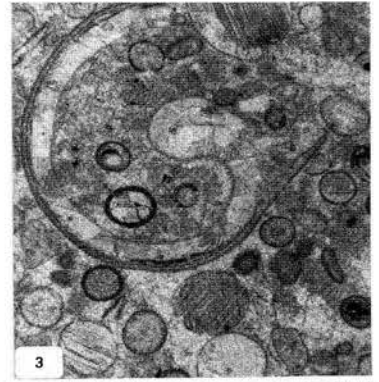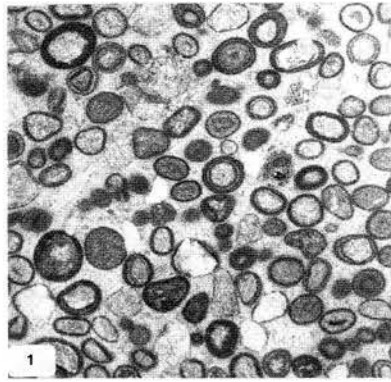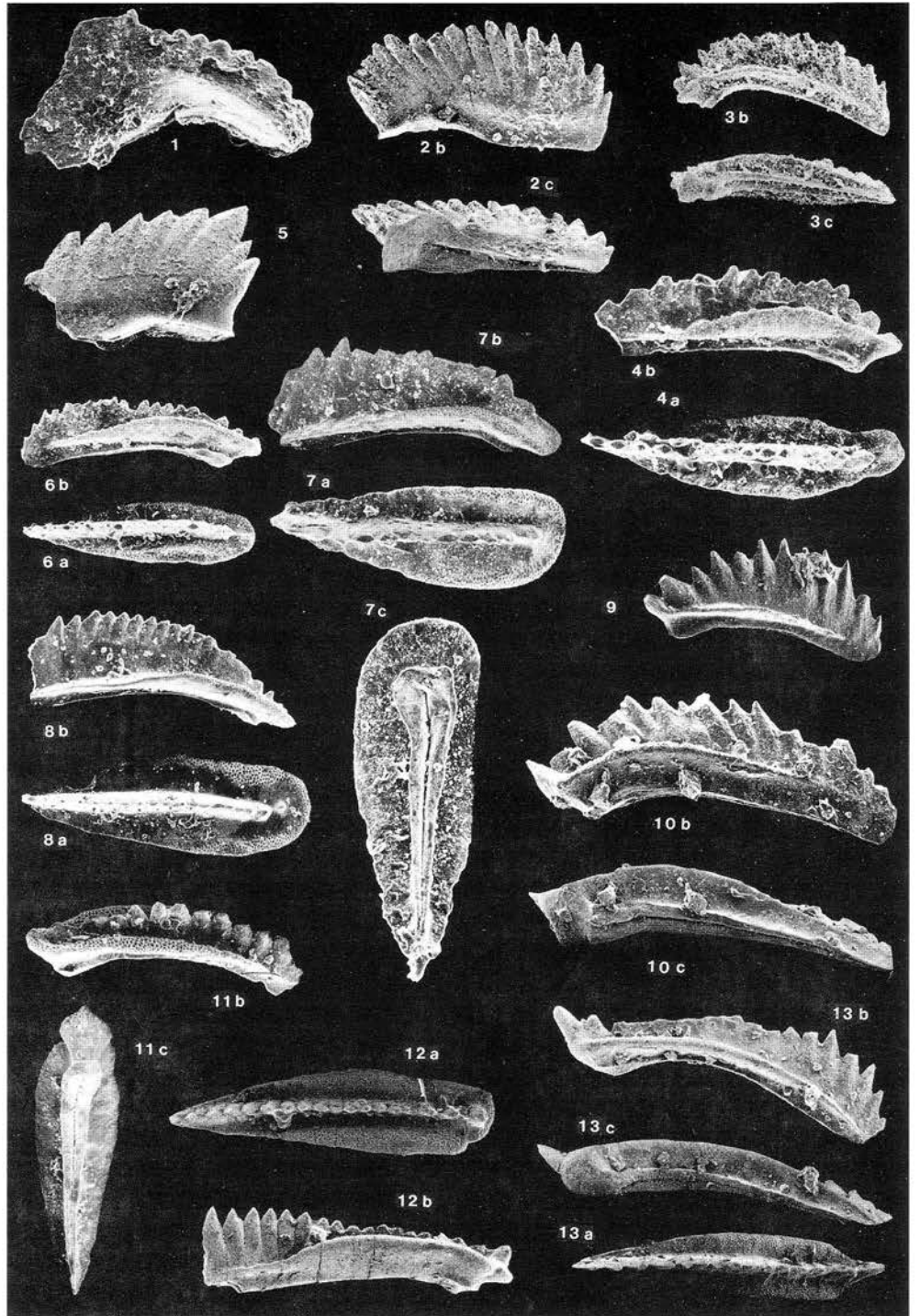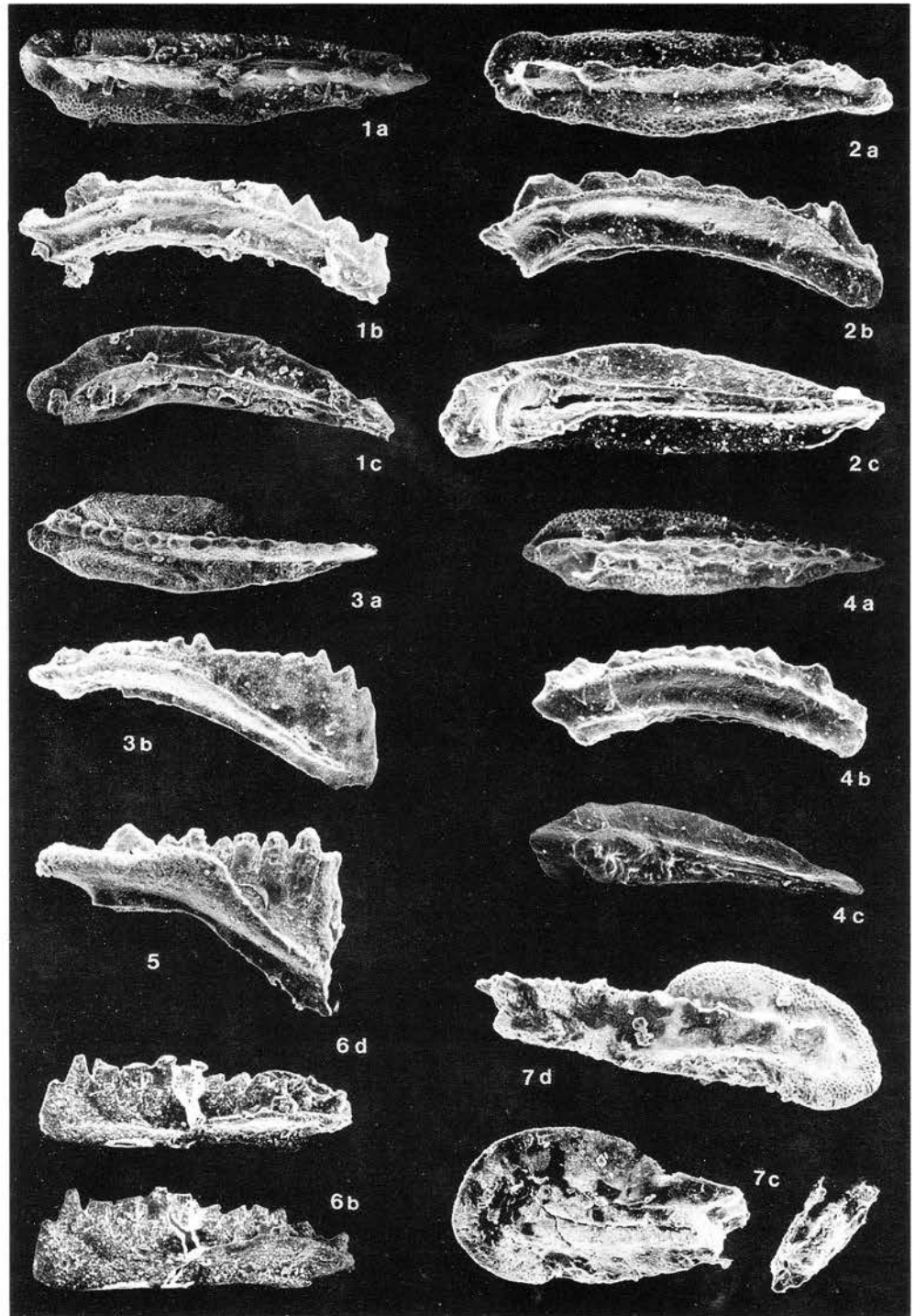
GEOLOGICAL MAP OF HYDRA ISLAND

L. Angiolini, L. Dragonetti & G. Muttoni

0   1 km

N. Alexandròs

N. Pontikòs

K. Bìsti

O. Ag. Nikòlaos

N. Petàsi

N.Zìngri

Ag. Nikòlaos West

O. Zakòni

Gherakìna

Episkopi

Ag. Marina

O. Mòlos

N. Kivòtos

K. Ag. Ioànnu

O. Farù

N. Palàmida

Nisìsa

N. Fòca

N. Kamìni

N. Kamìni

Vlichos

Kamìni

Hydra Chòra

O. Korufà

O. Eros

Pgf. Ilia

O. Pùrgos

O. Kontària

O. Màlies

Ag. Maròmes

Ag. Triàdos

O.Mandràki

Ag. Paraskeiù

O. Limniònisa

Ag. Pètros

K. Zingàri
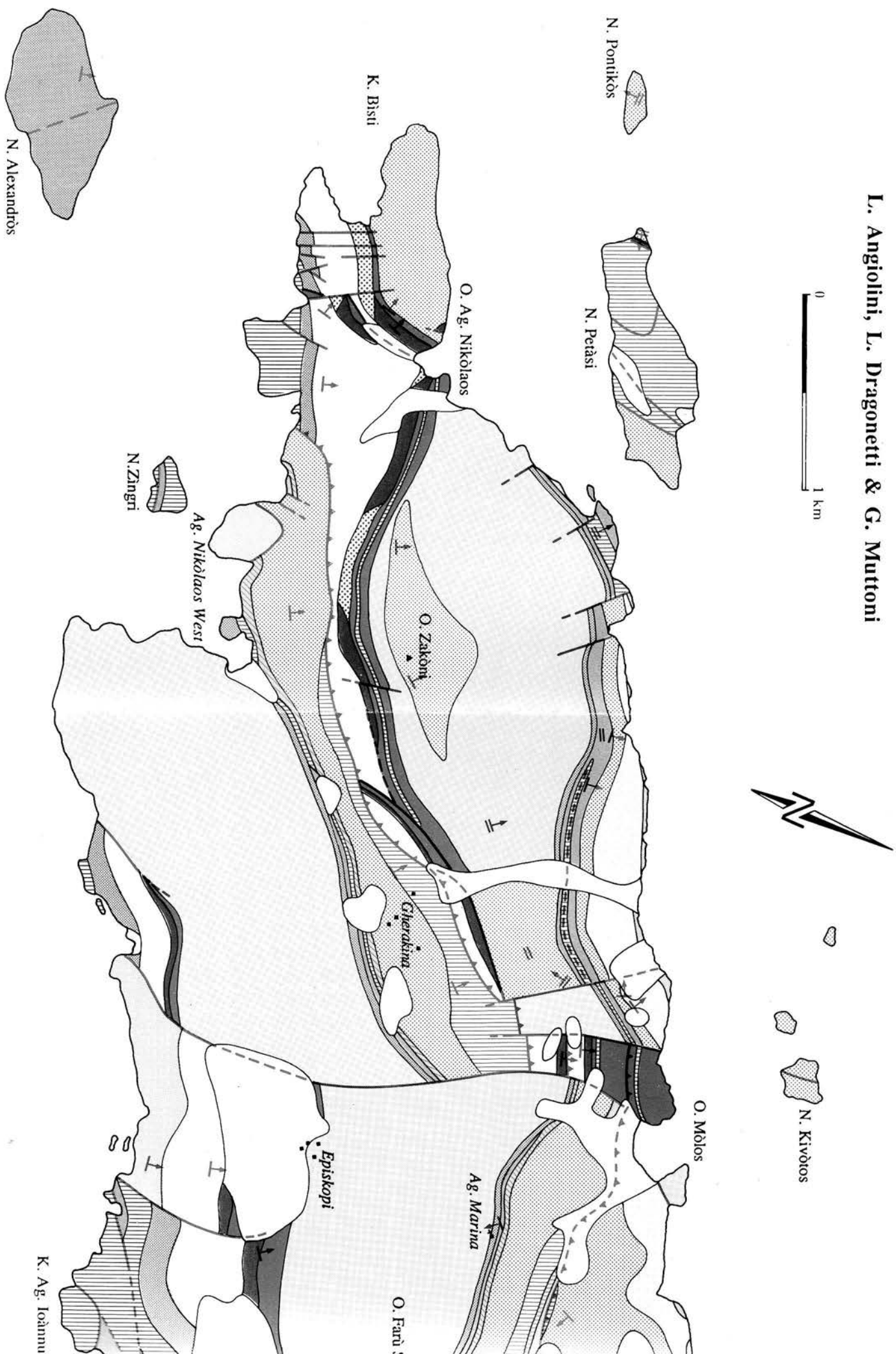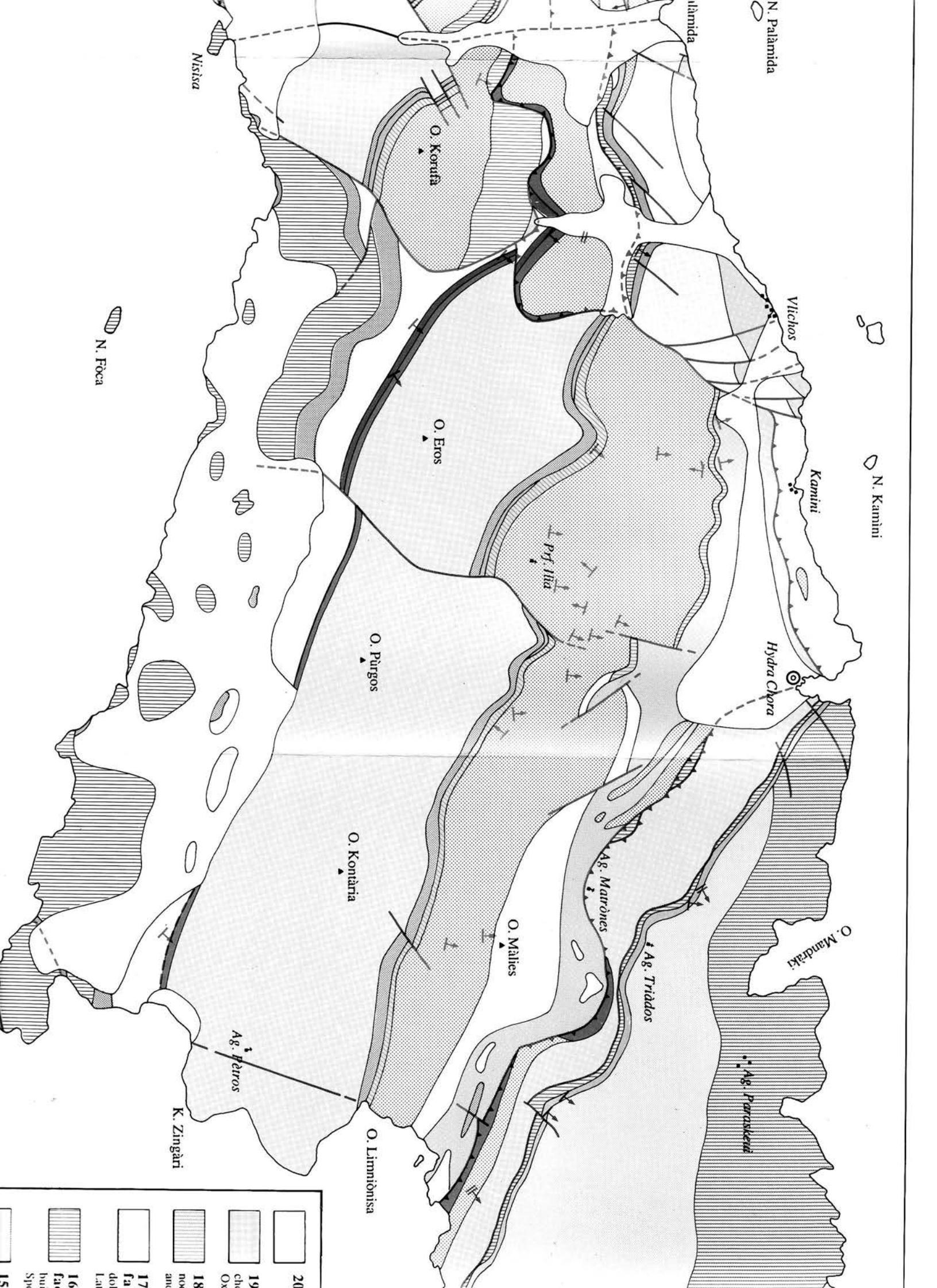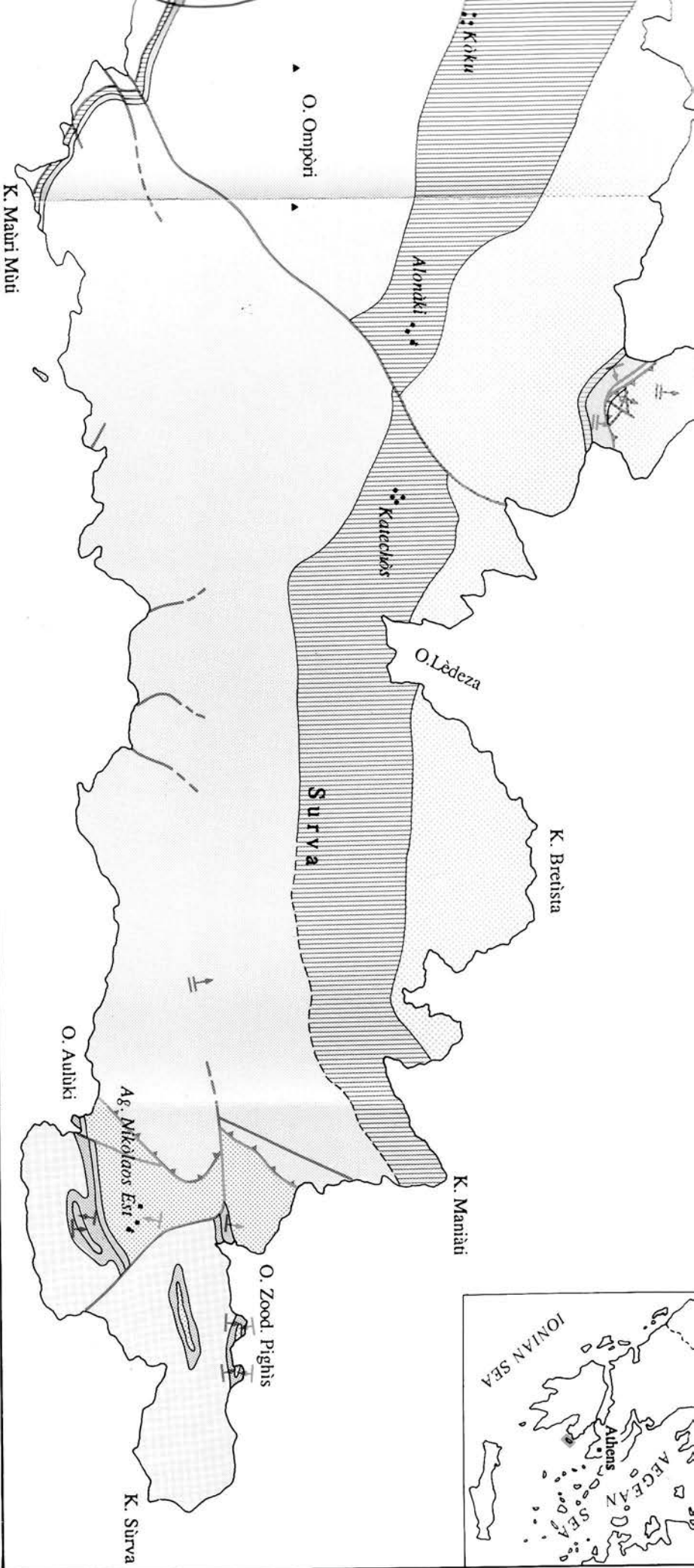
Radiolarites Fm: thin bedded red cherts with marls and silty marls. ?Aalenian-?Oxfordian.

Ammonitico Rosso Lmst: red nodular limestones with Ammonoids. Middle ?Late Early Jurassic.

Pantokrator Lmst, loferitic facies: bedded limestones with white dolomitic levels and contraction structures. ?Late Norian-Raethian.

Pantokrator Lmst, recifal facies: massive limestones with biohermal buildups mainly formed by Corals and sponges. (Ladinian) Carnian/Norian.

Pantokrator Lmst, biodetrital facies: slightly bedded detrital limestones. ?earliest Anisian/earliest Ladinian - Carnian.

K. Maùri Mùti

14 Pantokrator Lmst, resedimented Malies facies: massive biodetrital limestones.?Illyrian- Late Triassic.

13 Adhami Lmst, upper mb: thick bedded limestones with cherty nodules. Late Triassic.

12 Adhami Lmst: well bedded cherty limestones. ?Ladinian - Carnian.

11 Adhami Lmst, lower mb: thin bedded red cherts with limestones lenses and green cherts. Illyrian - ?Ladinian.

10a Quartz keratophyric tuffs: green tuffs, sometimes silicized. Pelsonian.

10 Han-Bulog Lmst: red and grey nodular limestones with ammonoids. Late Pelsonian - earliest Ladinian.

9 Eros Lmst, upper lithozone: limestones breccias with red matrix. Upper Pelsonian.

8a Eros Lmst, dark mb: dark, thin bedded wackestones. Spathian - Pelsonian.

8 Eros Lmst ss: massive ooïtic grainstones and packstones with Foraminifers. Spathian - Pelsonian.

7a Eros Lmst, basal silty beds: green siltstones with bivalvs. Spathian

7 Eros Lmst, lower lithozone: bedded oolitic grainstones with quartz grains.

6a Ag. Nikòlaos Fm, silty mb: yellow siltstones. Scythian.

6 Ag. Nikolaos Fm: bedded quartzarenites and quartzwackes. Scythian.

5a Episkopi Fm, Petàsi mb: massive packstones with bioclasts.

5 Episkopi & Miras Fms: well bedded packstones with Foraminifers, Corals, Brachiopods (Ep) and arkoses at the top (Mr). Dzhulfian - Dorashamian.

4a Marmari Fm: well bedded wackestones and packstones with Foraminifers.

4 Cap Bisti Gr pp: red sandstones and shales with dolomitic limestones.

3 Thikia Gr pp: bedded algal boundstones and packstones with Fusulinids.

2 Nisisa Fm: conglomerates, shales, with calcareous levels. Sakmarian.

1 Recrystallized Lmst: ?Palaeozoic.

O. Onpòri

Kòku

Alonàki

Katochòs

O.Lèdeza

S u r y a

K. Breísta

K. Maniàti

O. Aulùki

Ag. Nikòlaos Est

O. Zood. Pighìs

K. Sùrva

IONIAN SEA

AEGEAN SEA

Athens